Circuits and Systems
Mekelweg 4,
2628 CD Delft
The Netherlands
http://ens.ewi.tudelft.nl/

CAS-2010-02

M.Sc. Thesis

Multiuser Detection for Sensing Asynchronous LED Illumination Contributions

Deheng Liu B.Sc.

Abstract

In recent years, light-emitting diodes (LEDs) have played an increasingly more important role for light illumination. Beyond the basic function of pure illumination via intensity control of fixed color light, LED technology additionally allows control over the light color and illumination pattern. In order to realize these functions of intelligent lighting control, we need to estimate the light intensity of each LED in the sensor location. To this end, a synchronous code-time division multiple access - pulse width modulation (CTDMA-PWM) system [1] has been proposed for LED identification and simultaneous measurement of illumination strength. However, this system strictly requires perfect synchronization, which in practice is not easy to be guaranteed. Therefore, in this thesis, we propose an asynchronous CTDMA-PWM scheme and corresponding multiuser detection algorithm to combat the multiple access interference (MAI) caused by asynchronous multiple access. We explore the algorithm of conventional minimum mean square error (MMSE) linear estimation and implement it iteratively in a blind way without the knowledge of channel input from interfering LEDs.

Multiuser Detection for Sensing Asynchronous LED Illumination Contributions

Thesis

submitted in partial fulfillment of the
requirements for the degree of

Master of Science

in

Electrical Engineering

by

Deheng Liu B.Sc.
born in Wuhan, P.R.China

This work was performed in:

Circuits and Systems Group
Department of Microelectronics
Faculty of Electrical Engineering, Mathematics and Computer Science
Delft University of Technology

Delft University of Technology
Department of
Microelectronics

The undersigned hereby certify that they have read and recommend to the Faculty of Electrical Engineering, Mathematics and Computer Science for acceptance a thesis entitled **"Multiuser Detection for Sensing Asynchronous LED Illumination Contributions"** by **Deheng Liu B.Sc.** in partial fulfillment of the requirements for the degree of **Master of Science**.

Dated: 22-04-2010

Chairman: _____
Prof. Dr. ir. Alle-Jan van der Veen

Advisor: _____
Dr. Geert Leus

Committee Members: _____
Dr. ir. Gerard Janssen

_____
Dr. Hongming Yang

Abstract

In recent years, light-emitting diodes (LEDs) have played an increasingly more important role for light illumination. Beyond the basic function of pure illumination via intensity control of fixed color light, LED technology additionally allows control over the light color and illumination pattern. In order to realize these functions of intelligent lighting control, we need to estimate the light intensity of each LED in the sensor location. To this end, a synchronous code-time division multiple access - pulse width modulation (CTDMA-PWM) system [1] has been proposed for LED identification and simultaneous measurement of illumination strength. However, this system strictly requires perfect synchronization, which in practice is not easy to be guaranteed. Therefore, in this thesis, we propose an asynchronous CTDMA-PWM scheme and corresponding multiuser detection algorithm to combat the multiple access interference (MAI) caused by asynchronous multiple access. We explore the algorithm of conventional minimum mean square error (MMSE) linear estimation and implement it iteratively in a blind way without the knowledge of channel input from interfering LEDs.

Acknowledgments

I would like to thank my advisor Dr. Geert Leus for his great guidance and constant support for my thesis project. During my time in Delft, he showed me how to be a good teacher and a great researcher, through whom I learned how to conduct research in the area of signal processing for communication which led to this thesis. I also sincerely appreciate Dr. Tim Schenk in Philips Research Eindhoven for giving me the opportunity to undertake this thesis project. Many thanks to Prof. Dr. Alle-Jan van der Veen, for the time he spent with me in discussing and helping me to solve problems. Besides, significant appreciations will be given to Dr. Gerard Janssen, who nominated me as a candidate for the HSP Huygens Scholarship, which covered my tuition fee and living cost in Delft. This thesis has been possible because of their support, encouragement, understanding and friendly attitude.

Special thanks to my parents and my beloved wife, Xiao Zhang, who supported me no matter what kinds of difficulties I had during my master program. Thank you for surrounding me and supporting me with love. Eventually, my gratitude to all my friends in Delft and Eindhoven: Daoxin Li, Xiaolei Cui, Sijie Chen, Guang Ge, Chi Liu, Ruiming Yang, Xiaodong Guo, Tianyi Zhang, Xing Xu and my friends since Childhood: Wanxing Zhan and Zhe Cong, thank you for your help and the time being together.

Deheng Liu B.Sc.
Delft, The Netherlands
22-04-2010

Contents

List of Figures

List of Tables

1 Introduction

1.1 Background

Light-emitting diodes (LEDs) present many advantages over traditional light sources including low energy consumption, longer lifetime, improved robustness, smaller size and fast switching. Therefore, in recent years, LED technology has emerged as a prime candidate for future illumination light sources. Beyond the basic function of pure illumination via intensity control of the fixed color light, LED technology additionally allows control over the light color and illumination pattern. By using these techniques, the new idea of an intelligent lighting system [1], which was proposed by the Distributed Sensor System (DSS) Department in Philips Research Eindhoven, aims to shift the basic function of pure illumination into dynamic lighting atmosphere positioning. Previous work in the DSS Department in Philips Research Lab has developed a new family of modulation methods (pulse position modulation and pulse width modulation), a hybrid synchronous multiple access scheme (code-time division multiple access) and corresponding illumination estimation algorithms to accurately measure and estimate the local light contribution of a large number of LED light sources. Based on these algorithms, a demo has been made to demonstrate multiple functions of an intelligent lighting control system. It is believed that this kind of smart and intuitive control of a lighting system will be essential for a successful market entry.

1.2 Motivation

In the proposed two-dimensional multiple access system, a synchronous code-time division multiple access (CTDMA) scheme by employing orthogonal Walsh-Hadamard (WH) codes are used to guarantee the perfect orthogonality and allow for a computationally efficient multi-signal receiver algorithm.

However, in this scheme, perfect synchronization of the LED light sources is highly demanded, which causes additional infrastructure in the lighting system. Moreover, in a practical lighting system, certain timing inaccuracy between the different light sources and between the light sources and the sensor is inevitable, which will result in estimation errors. Building up on this analysis, in this thesis, I will perform my research on the study of a new asynchronous two dimensional code-time division multiple access scheme and corresponding algorithm investment to tackle the multiple access interference (MAI) caused by an asynchronous code division multiple access scheme.

As one of the candidates for the MAC layer multi-access technologies, ALOHA has been adopted to solve aforementioned problems [2]. However, a responding time of approximately 30 seconds is needed for a sensor receiver to be able to estimate the light intensity. Apparently, this is not satisfied for the requirement of a real-time lighting

control system. Motivated by the analysis above, a code-time division multiple access scheme and advanced signal processing techniques for detection and estimation are expected to be applied in the receiver for a better system performance.

1.3 Intelligent Lighting Control System Architecture

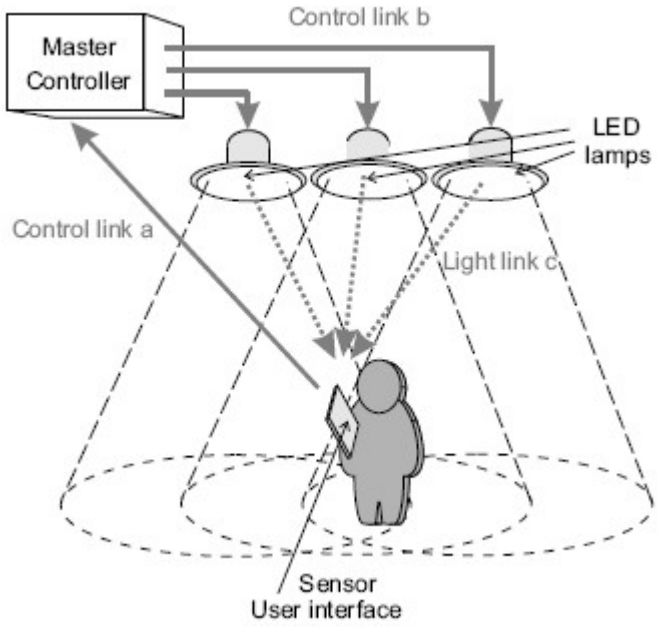

Figure 1.1: Intelligent lighting control system architecture

Figure 1.1 [1] [3] depicts the system architecture of the proposed intelligent control system. As can be seen from the figure, a control loop is formed via three links in between different components of the lighting system. A large number of LED lamps are located on the ceiling and connected with the external master controller through a bi-directional "control link b", which could be either a wired link or radio frequency (RF) wireless link. The user holds a remote controller (receiving sensor) in the location where he receives the tagged signal emitted from arrays of LEDs through an uni-directional "light link c" and estimates the light intensity in the sensor location. One can input the required lighting pattern, through typing the request information in the control panel of the user interface to control the desired lighting effect, such as burning hours or lamp temperature,etc. Afterwards, the input information coupled with the estimated light intensity will be transmitted to the master controller via "control link a". "control Link a" can also be a bi-directional RF link, for instance, ZigBee radio link or an IR link. Through the loop in the figure, the data will be processed in the master controller and then be delivered to each LED via "control link b". Accordingly, the lighting system can automatically figure out the "light contribution of each light source and modify the light setting in demand. In this thesis, I will concentrate on the link c", which is the illumination propagation path. Multiple uniquely "coded

lights" are modulated, transmitted over the air, and impinge on the receiving sensor simultaneously. The sensor at the user location will receive the tags embedded by LEDs and estimate the light intensity of each LED at the sensor location. From the above description, we can see that it is very important for the user to have a real time interactive experience, which requires a practical, convenient and efficient approach for data modulation, multiple access and intensity estimation.

1.4 System Requirement

In the project, there are a set of requirements posted on the modulation and multiple access schemes for the light link and the corresponding estimation algorithms. These requirements are listed in the following:

a) Number of Lamps: In this project, the number of lamps will be set in between one hundred and one thousand. This is because, in practice, several hundreds of LEDs are enough for both illumination and intelligent lighting control within a room. Moreover, if the number exceeds one thousand, the complexity of the system will be further increased. To make things easier, we will consider the number of LEDs in the scale of hundred in this project.

b) Detection and Estimation Time: To take the feasibility and practical need into consideration, the response time is preferred to be within two seconds. This means when the user presses the button on the control panel of the user interface, he or she is able to get the desired lighting control effect within 2 seconds. In this project, time spent on other aspects are much less than the detection and estimation time, thus can be neglected. Therefore, we will consider the time spent on detection and estimation as the primary responding time.

c) Compatible Modulation Method: The data modulation method should be compatible to the commonly used Pulse Width Modulation (PWM) method of controlling the intensity and color point of the LED.

d) Asynchronous Transmission: The significant improvement of this project is to consider an asynchronous transmutation system. As we know from previous research results and analysis, due to the timing inaccuracy in the practical lighting system, the LED light sources cannot be perfectly synchronized all the time, which will degrade the system performance dramatically. More importantly, extra infrastructure is highly demanded for each LED to guarantee synchronous transmission. In an intelligent lighting control system, thousands of LEDs are needed. Due to the extra efforts for synchronizing each LED, the cost will be increased substantially. Consequently, it is very important to design a novel asynchronous multiple access scheme to be able to use a more conventional system.

e) Estimation Accuracy: There is one important parameter to assess the estimation algorithms that are employed. Lower estimation error is desired. To achieve this goal, a variety of estimation methods will be investigated.

f) Invisible Modulation: Although we are aiming to achieve a smart control of the lighting system, the basic function of illumination cannot be ignored. Specifically, the modulation scheme and the lighting dimming method should not cause visible flickering. Therefore, the low frequency components from 0 Hz to a few hundreds Hz have to be eliminated.

g) Other Requirements: the requirements listed above are the most important requirements. If all the these can be satisfied, some additional requirements, such as energy efficiency and low complexity can be further considered to improve the system performance.

1.5 Outline and Contributions

In this section, I will first describe the content of the thesis chapter by chapter, and then briefly summarize our major contributions. The main content of each chapter is outlined as follows

Chapter 1: Introduction

This chapter gives an introduction to the background of this thesis project. Afterwards, it presents the motivation to perform the research of the asynchronous transmission and raises the problems of multiple access interference, which needs to be suppressed in the following chapters. Moreover, it also describes the system architecture in the proposed lighting system and briefly gives the system requirements.

Chapter 2: System Model

In this chapter, we present a literature study of previous research [1] [3] [4] that has been undertaken in the DSS department of Philips Research Eindhoven. We review the proposed modulation method and extend the synchronous multiple access scheme to the asynchronous mode. Moreover, various channel disturbances are modeled and derived to obtain a clear system data model. Note that part of the content in this chapter appears in [1] and [3].

Chapter 3: Asynchronous Receiver Design

This chapter contains the major contribution of the thesis. First, we derive the data model for the asynchronous receiver. Then, the conventional minimum mean square error (MMSE) linear multiuser detector is presented to solve the problem under the assumption that we have full knowledge of the timing references and spreading codes of all LEDs in the system. Subsequently, a blind adaptive linear MMSE detector by using the Least Mean Square (LMS) optimization algorithm is derived to give a sensible solution without requiring the information from other interfering LEDs. Finally, the numerical results of both conventional and blind MMSE detectors are presented based on a typical indoor scenario.

Chapter 4: Imaging Diversity

In this chapter, we propose a new idea of imaging diversity to provide an optical so-

lution. Basic lens design is conducted and the result might be useful for further research.

Chapter 5: Conclusions and Further work

This chapter summarizes the main ideas of the thesis and gives suggestions for further research regarding this topic.

2 System Model

In this chapter, we will describe the system model of the considered intelligent lighting control system. Section 2.1 introduces a modulation method of LEDs - Pulse Width Modulation (PWM) to identify and control the intensity of LED lighting. Section 2.2 gives an idea of the asynchronous multiple access scheme. In section 2.3, the channel model of the "light link c" will be presented, and different noise and disturbance will be discussed.

2.1 Modulation

In order to deliver different illumination levels, LEDs are typically driven with repeatedly transmitted pulses whose widths are modulated [5], using so-called Pulse Width Modulation (PWM). In this section, we will study the illumination adopting the PWM modulation method. A three layer structure (slot, block and frame) is introduced to describe the modulated pulse waveform.

- A slot is the smallest time unit in this three layer structure scheme and represents the clock timing at which the power LEDs are driven. It has a duration of T_1, which is the resolution at which the LEDs can be modulated.
- A block represents one chip and has duration $T_2 = N_1 T_1$, which is shown in Figure 2.1. N_1 is the number of possible adjustments for the duty cycle for dimming purposes. Accordingly $\log_2 N_1$ represents the dimming capacity. A block duration is the time unit where one pulse is emitted by one LED light.
- A frame is the top layer of the modulation scheme. Its duration can be given by $T_3 = N_2 T_2$. It is the time interval where one identifier (ID) is transmitted and one measurement of the illumination intensity of each LED is made. Therefore, T_3 is a very important system parameter, since it is the processing time that the receiver sensor spends to identify and measure all relevant light sources. In my project, one of the main objects is to reduce the responding time T_3 in order to provide users an immediate reaction after pressing a control button.

In the following, we will introduce the block and frame modulation format respectively by employing the binary PWM modulation scheme.

2.1.1 Block Modulation Format

In this section, we introduce the binary PWM for a pulse of amplitude A_l and timing reference $\tau_l \in \{1, 2, ..., N_1\}$, where l stands for the LED index. Next, a non-modulated pulse and pulse width modulation (PWM) will be shown respectively.

1) Non-modulated pulse

Figure 2.1 depicts a non-modulated driving pulse waveform, from which we can see that the starting position of all pulses for the lth LED equals τ_l. The pulse width in terms of number of slots is given by

$$w_l = \lfloor pp_l N_1 \rceil \tag{2.1}$$

where $\lfloor \cdot \rceil$ represents the nearest integer and $(1 - pp_l)$ is the dimming level of the lth

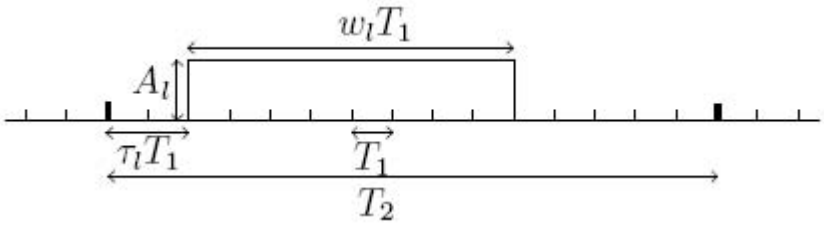

Figure 2.1: Non-modulated pulse waveform

LED, with the duty cycle $0 \leq pp_l \leq 1$. Note that the dimming level is a parameter that can be different for different LEDs.

2) Pulse width modulation (PWM)

Fig 2.2 illustrates a PWM waveform.

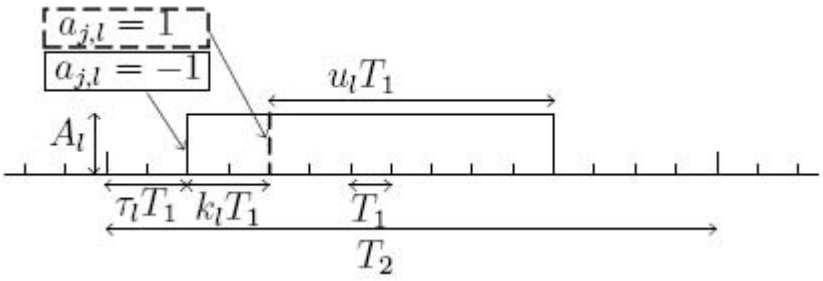

Figure 2.2: Pulse width modulation pulse waveform

The starting position of the jth pulse for the lth LED, with $j = 0, 1, ..., N_2 - 1$ and $l = 1, 2, ..., L$ is given by

$$\delta_{j,l} = \begin{cases} \tau_l & a_{j,l} = -1 \\ \tau_l + k_l & a_{j,l} = 1 \end{cases} \tag{2.2}$$

where τ_l and k_l are the allocated time slot and the modulation depth for the lth LED, respectively, and j denotes the jth chip of the spreading sequence or identification code for the lth LED. Further

$$a_{j,l} = b_l \, c_{j,l} \tag{2.3}$$

where $b_l \in \{+1, -1\}$ is the information bit from the lth LED and $c_{j,l}$ denotes the jth chip of the spreading sequence with $c_{j,l} \in \{+1, -1\}$. The length of the spreading sequence is N_2. In our project, we can control the transmission data that we want to send. In this case, we can assume that all the transmission bits equal 1, thus $b_l = 1, \forall l$. Therefore

$$a_{j,l} = c_{j,l} \tag{2.4}$$

which means that $a_{j,l}$ can also represent the spreading code. In order to figure out where the pulse ends, it is also valuable to define the pulse width:

$$w_{j,l} = \begin{cases} u_l + k_l & a_{j,l} = -1 \\ u_l & a_{j,l} = 1 \end{cases} \tag{2.5}$$

where $u_l = \lfloor pp_l N_1 - k_l/2 \rceil$ to assure no loss of the total light energy. From Figure 2.2 we can also see that the pulses end at $\{\tau_l + k_l + u_l\} \, mod \, N_1$ regardless of $a_{j,l}$. This means that $w_{j,l}$ depends not only on the required light level but also on the spreading sequence.

2.1.2 Framing

Figure 2.3 shows the two-dimensional framing process. An example of a pulse train of one frame is illustrated. The hatched grid points represent the coded light with full energy, while the blank grid points mean no signal in the corresponding slots. In this frame, $N_1 = 10$, $N_2 = 4$, and the code $\mathbf{a}_l = [-1, 1, -1, 1]^T$ is applied. As indicated in the figure, timing reference $\tau_l = 2$, modulation depth $k_l = 2$ and dimming duty cycle $pp_l = 0.5$. By using these parameters, we can calculate $u_l = \lfloor pp_l N_1 - k_l/2 \rceil = 4$. As a result of this, the pulse width $w_{j,l}$ can be easily derived.

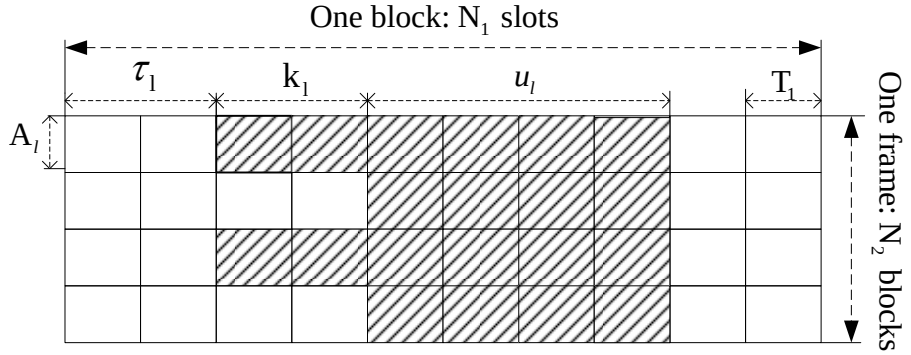

Figure 2.3: Framing

In fact, different blocks will be transmitted one by one along the time axis, however, in this figure, they are stacked on top of each other to provide a clear view of the spreading process. We consider the driving signal for the lth LED and omit the notation details of pulses extending into neighboring blocks. Thus one frame of a continuous

sequence of repetitive frames can be expressed as:

$$s_l(t) = \sum_{j=0}^{N_2-1} \sum_{n=0}^{N_1-1} s_{j,n,l} \prod \left(\frac{t - jT_2 - nT_1}{T_1} \right) \tag{2.6}$$

Here n and j refer to the positions of the slots in a block, and to blocks in the frame respectively. $\prod(t) = U(t) - U(t-1)$ is the unit pulse of unit width and amplitude, where $U(t)$ is the unit step function. $s_{j,n,l}$ represents the sample of $s_l(t)$ at $t = jT_2 + nT_1$ For the case of PWM, it is given by

$$s_{j,n,l} = \begin{cases} 0 & n = 0, 1, ..., \tau_l - 1 \\ \frac{1-a_l}{2} & n = \tau_l, ..., \tau_l + k_l - 1 \\ 1 & n = \tau_l + k_l, ..., \tau_l + u_l + k_l - 1 \\ 0 & n = \tau_l + u_l + k_l, ..., N_1 - 1 \end{cases} \tag{2.7}$$

These pulses consist of a code-carrying prefix and a main illumination pulse. The prefix code uniquely identifies the information from each LED.

2.2 Asynchronous Multiple Access

A lot of research has been performed on the modulation and multiple access scheme of visible light communications. In recent years, they are mainly for code division multiple access (CDMA) for multiple user infrared (IR) communication systems [6][7]. In our proposed visible light communication link, in order to achieve high speed data communication with an array of LEDs, techniques compatible with the commonly used PWM light dimming techniques are being adopted, such as orthogonal frequency division multiplexing (OFDM) [8], which can be used to modulate a system/array of data signals on all LEDs. However, our project aims to estimate the illumination contribution individually for each LED, which means OFDM can not be applied directly. To this end, a CDMA scheme is considered as a multiple access scheme so that the light sources can be distinguished individually within the aggregate illumination and their individual contributions can be estimated regularly, accurately and simultaneously. - Show quoted text -

In my thesis, instead of the conventional CDMA scheme, we define a two dimensional multiple access system, namely code-time division multiple access (CTDMA). This is also compatible with the three layer modulation method we proposed in the previous section. As shown in Figure 2.3, different dimming level is imposed in the horizontal direction, while in the vertical direction, the data source from the lth LED is spreaded by using CDMA. We propose to use Walsh-Hadamard (WH) codes excluding the first code, since they provide balanced "1" and "-1", which may give some convenience in the further processing. In addition, this balanced property fixes the frame-average duty cycle and shapes the illumination spectrum to make the data imperceivable. Furthermore, the system becomes resilient to sources of constant of sufficiently slowly varying interfering light sources such as sunlight or incandescent bulbs. The spreading code

assigned to the lth LED is

$$\mathbf{c}_l = \mathbf{d}_{\gamma_l} = [d_{0,\gamma_l},\ d_{1,\gamma_l}, ..., d_{N_2-1,\gamma_l}]^T \tag{2.8}$$

which corresponds to the γ_lth WH code, with $\gamma_l \in \{2, 3, ..., N_2\}$. Here $\gamma_l \neq 1$ since we have excluded the first WH code. Because $b_l = 1\ \forall l$, $\mathbf{a}_l = \mathbf{c}_l$ also represents the spreading code of the lth LED.

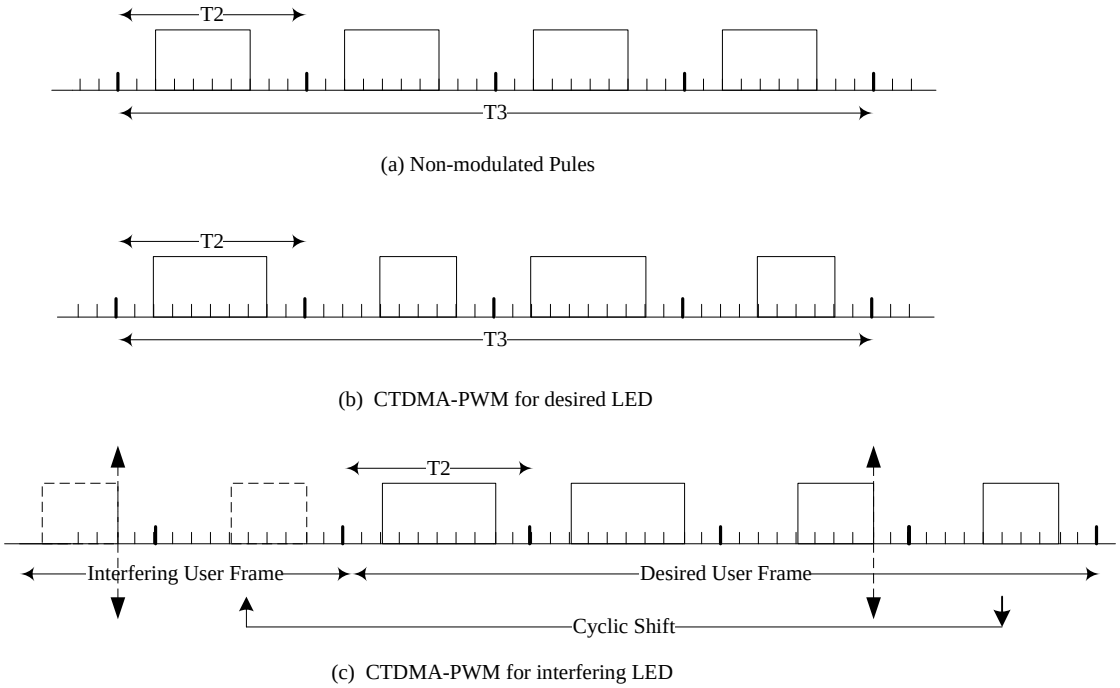

Figure 2.4: Pulse train for one frame in the asynchronous multiple access scheme

Next, we will start to learn the asynchronous multiple access scheme from one simple example given by Figure 2.4, which illustrates the pulse train for one frame of the desired LED and interfering LEDs in an asynchronous multiple access scheme. As shown in Figure 2.3 (b), the system adopts the same parameters as Figure 2.3 does. Specifically, WH code $\mathbf{a}_l = [-1, 1, -1, 1]^T$ for the desired user, timing reference $\tau_l = 2$, modulation depth $k_l = 2$ and dimming duty cycle $pp_l = 0.5$. Figure 2.4 (b) depicts the bit stream of Figure 2.3, and Figure 2.3 (c) describes an interfering LED, say $\tilde{l}$th LED, with WH code $\mathbf{a}_{\tilde{l}} = [-1, -1, 1, 1]^T$ and the timing reference $\delta_{\tilde{l}} = 2 + N_1 + 2 = N_1 + 4$. From this example, it can be seen clearly that in order to describe an asynchronous multiple access scheme, it is important to define the timing reference $\delta_{\tilde{l}}$ of the $\tilde{l}$th LED, which can be considered as the interfering user for the lth LED. $\delta_{\tilde{l}}$ is given by

$$\delta_{\tilde{l}} = \tau_l + p_{\tilde{l}} N_1 + q_{\tilde{l}} \tag{2.9}$$

where $q_{\tilde{l}}$ defines additional timing offset per time slot and $p_{\tilde{l}}$ represents the timing shift per block. $p_{\tilde{l}} N_1 + q_{\tilde{l}}$ provides the information of the additional timing reference, hence each combination $(p_{\tilde{l}}, q_{\tilde{l}})$ uniquely gives the information of the starting

position of the coded signal from an interfering user. Therefore, in Figure 2.3 (c), $p_{\tilde{l}} = 1$ and $q_{\tilde{l}} = 2$ if we assume the intentional timing $\tau_l = 2$. Further, in equation (2.9), $p_{\tilde{l}} \in \{-N_2 + 1, ..., 0, ..., N_2 - 1\}$ and $q_{\tilde{l}} \in \{-\tau_l, ...0, ...N_1 - \tau_l - 1\}$, so that $(\tau_l + q_{\tilde{l}}) \in \{0, ...N_1 - 1\}$. Normally, we have the knowledge of the intentional timing from the interference signal, which means τ_l is known to the receiver. In this case, if $(p_{\tilde{l}}, q_{\tilde{l}})$ is assumed to be known, we know the starting position of the interfering LED, which can be considered as a precondition to apply the conventional MMSE linear detector in section 3.2. Due to the asynchronous transmission, the multiple access interference (MAI) is prominent and largely jeopardizes the system performance. To solve this problem, different approaches with advanced signal processing techniques will be proposed and presented analytically and numerically in the subsequent chapters.

2.3 Channel Model

Figure 2.5 shows the system block diagram. $s_l(t)$ represents the output of the lth LED driver, while $y_m(t)$ denotes the output the mth sensor. The corresponding optical transmit and receive signals are denoted in the figure as $\varsigma_l(t)$ and $\chi_m(t)$ respectively. In the proposed lighting system, only one photodiode (PD) receiver is used, hence we can omit the index m.

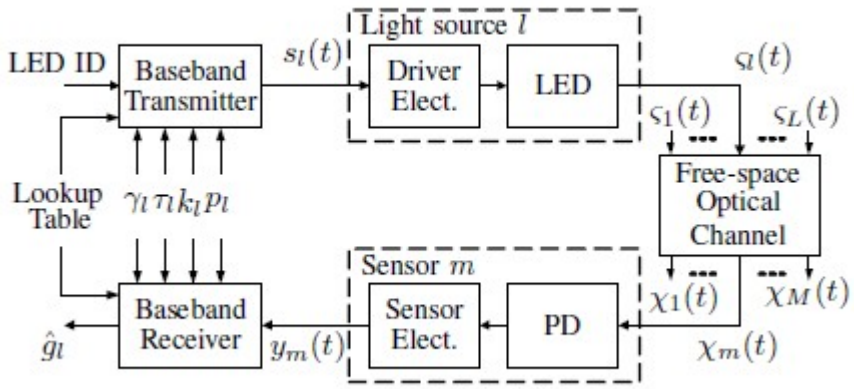

Figure 2.5: System block diagram

2.3.1 Electro-Optical Conversation

The optical transmit signal $\varsigma_l(t)$ in response to a step function of the electrical transmit signal is $\varsigma_l(t) = A_l \eta_l h_{on}(t)$ [9] where η_l denotes the LED responsivity. The unit step response of LEDs looks approximately as an exponential function [10], i.e.:

$$h_{on}(t) = U(t)[1 - \exp(-\mathrm{t}/\tau_{\mathrm{on}})], \tag{2.10}$$

$$h_{off}(t) = 1 - U(t)[1 - \exp(-\mathrm{t}/\tau_{\mathrm{off}})]. \tag{2.11}$$

The time constants τ_{on} and τ_{off} for on- and off-switching tend to differ [11]. Ignoring a possibly more complicated interaction between the on- and off-tails for very short pulses, the CTDMA-PWM optical signal becomes

$$\varsigma_l(t) = \sum_{j=0}^{N_2-1} A_l \eta_l h_{on}(t - jT_2 - \delta_{j,l}T_1) h_{off}(t - jT_2 - (\delta_{j,l} + w_{j,l})T_1) \tag{2.12}$$

2.3.2 Indoor light propagation

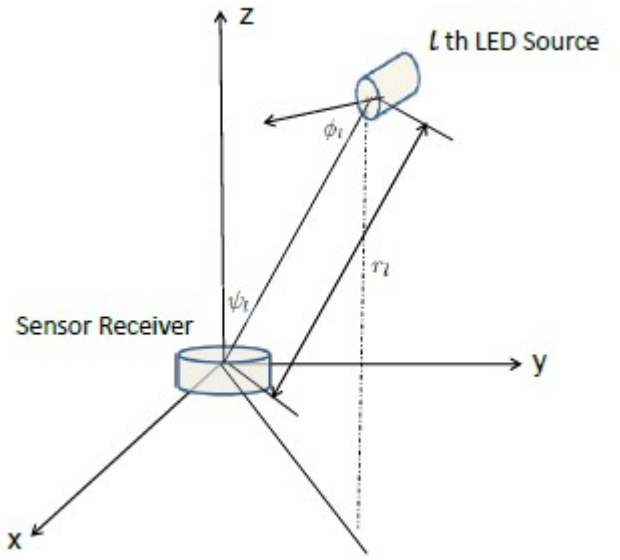

Figure 2.6: Geometry in LOS link calculating

The LED light reaches the receiver sensor via a directed path and possibly via multiple paths. However, for the typical commercial power LED, the slot time $T_1 \approx 1\mu s$, so that the inter-symbol interference(ISI) caused by the multipath propagation can be considered negligible. As shown in Figure 2.6 [12], in the proposed intelligent lighting control system, we model a line of sight (LOS) path with a photodiode (PD) receiver. It is easier to understand this if we consider the fact that narrow LED beams will contribute to the main illumination through the direct LOS path.

Based on the analysis above, we can derive the gain of the optical path:

$$\alpha_l = \frac{1}{r_l^2} R(\phi_l) \mathcal{A} \cos(\psi_l) \tag{2.13}$$

where r_l is the distance between the power LED and sensor receiver. $\mathcal{A}$ is the area of the photodiode (PD) and the angle ψ_l represents the orientation of LED l. We also define $R(\phi_l)$ the LED radiation pattern, which is assumed to be rotationally symmetric and includes the effects of the lens. Moreover, the angle ϕ_l is the angle with respect

to the transmitter surface normal. Thus $R(\phi_l)$ can be further modeled according to a generalized Lambertian law [13][9]

$$R(\phi_l) = \frac{\mu + 1}{2\pi} \cos^{\mu}(\phi_l) \tag{2.14}$$

where μ is the Lambertian mode number and $\mu = -ln2/ln(cos(\Phi_{1/2}))$, where $\Phi_{1/2}$ is called half-power semiangle. We assume the transmitter has a half-power semiangle $\Phi_{1/2}$ equal to 45 degrees, corresponding to $\mu = 2$.

2.3.3 Opto-Electrical Conversion

The PD at the receiver converts the optical signal into the electrical signal $y(t)$. Its responsivity is denoted by ϵ_l, which is color dependant, thus carries index l. The response speed of PDs is generally much higher than that of the power LED, hence, the switching effects can be considered negligible [9][14]. In my project, for simplicity, we assume that $\epsilon_l = \epsilon, \forall l$ since the color estimation is not addressed in this thesis.

2.3.4 Channel Disturbance

It is also important to know clearly the channel disturbance. In the considered lighting system, there are three major sources of disturbances. As it is an optical channel, two primary noises are additional Gaussian thermal noise and approximately Gaussian distributed short noise. In addition, the background light noise, which is treated as a constant DC bias, needs to be considered. In the following, we will model these disturbance and derive the received signal $y(t)$.

The background light consists of light contributions from other ambient sources, which in the envisaged LED lighting system would be mostly sunlight, if at all. Its power is denoted by $\zeta(t)$. Its fluctuation is assumed to be slower than T_3^{-1} thus can be approximated as DC during each frame. Therefore, the argument t is omitted. Furthermore, we expect the background light does not result in saturation of the receiver.

Electronics thermal noise is mostly created by the transimpedance amplifier for the PD signal, and predominantly behaves as additive Gaussian thermal noise. For a power spectral density (PSD) S_{th} $[A^2/\text{Hz}]$ and an effective bandwidth B_n, the variance for the thermal noise equals

$$\sigma_{th}^2 = S_{th} B_n \tag{2.15}$$

Shot noise is due to a stream of electrons that are generated at random times in the PD. It is approximately Gaussian distributed due to the central limit theorem [15]. The shot noise power σ_{shot}^2 is linearly proportional to all light shed on the PD surface, not only including the lights form LEDs, but also the background light. Hence it can be expressed as

$$\sigma_{shot}^2(t) = 2q_e B_n (\sum_{l=1}^{L} \alpha_l \epsilon_l \varsigma_l(t) + \epsilon_\zeta \zeta) \tag{2.16}$$

where q_e is the electrical charge of the electron and L represents the total number of LEDs in the system. As an approximation, we assume that the sum of all the lights

is time independent, e.g. due to strong background light. Hence the argument t of $\sigma^2_{shot}(t)$ will be dropped. Furthermore, we can also assume that $\epsilon_l = \epsilon_\zeta = \epsilon$, thus equation (2.16) can be rewritten as

$$\sigma^2_{shot} = 2q_e B_n \epsilon (\sum_{l}^{L} \alpha_l \varsigma_l + \zeta) \tag{2.17}$$

Based on the analysis of different types of Channel disturbance, we can derive the received electrical signal as follows:

$$y(t) = \sum_{l=1}^{L} \epsilon \alpha_l \varsigma_l(t) + v_\zeta + v_{th}(t) + v_{shot}(t) \tag{2.18}$$

where $v_\zeta = \epsilon\zeta$ denotes the background light contribution, while $v_{th}(t)$ and $v_{shot}(t)$ represent the thermal noise and the shot noise, respectively.

2.4 Conclusion

In this chapter, we have first introduced pulse width modulation (PWM) in section 2.1. A three layer modulation structure is studied. (2.6) and (2.7) give the expression of one frame, which is able to identify one LED. Then in section 2.2, we have discussed the research background and motivation for an asynchronous multiple access scheme. The problem of multiple access interference is presented, which can be considered as a guidance in the subsequent chapters. Section 2.3 derives the data model of different channel disturbances in the proposed system. Finally, (2.18) expresses the received signal in the sensor location.

3 Asynchronous Receiver Design

In this chapter, I perform the research on the asynchronous receiver design. In section 3.1, the receiver data model is derived for the asynchronous multiple access. Section 3.2 presents the MMSE solution for the proposed data model under the assumption that we know the timing of the spreading sequences of all users. In section 3.3, a minimum output energy (MOE) based blind adaptive approach is given and applied to solve the problem in case we only know the timing and the spreading code of the desired user. Section 3.4 specifies parameters in one scenario and gives the simulation results for conventional MMSE and blind adaptive MMSE, respectively.

3.1 Data Model of Asynchronous Receiver

The baseband receiver processing consists of the following main steps. In order to achieve a low complexity receiver implementation, we first apply integrate-and-dump (I&D) processing to the received signal to yield a discrete time signal. Afterwards, a linear estimator is used to find the illumination intensities for the different light sources.

The I&D receiver outputs the $N_2 \times N_1$ matrix $\mathbf{Y}$, whose (j, n)th element equals

$$\mathrm{Y}[j,\, n] = \frac{1}{T_1} \int_{jT_2+(n-1)T_1}^{jT_2+nT_1} y(t)dt \tag{3.1}$$

Hence, $\mathbf{Y}$ captures an entire frame of the desired user. As mentioned in chapter 2, we can assume without loss of generality that the coded light signal from the user of interest has an initial timing reference τ_l and modulation depth k_l. For further processing, we use a $N_2 \times k_l$ submatrix $\mathbf{Y}_l$, containing the columns $\tau_l, ..., \tau_l + k_l - 1$ of $\mathbf{Y}$, which are the spreaded data sequences of the lth LED. In the proposed asynchronous multiple access system, the initial timing reference of other users varies in the range of $[1, N_1 N_2]$ with equal probability. The multiple access interference is due to data sequences from asynchronous interfering users that fully or partially fall into the columns of $\mathbf{Y}_l$. This can be modeled as the following condition

$$\delta_{\tilde{l}} = \tau_l + p_{\tilde{l}} N_1 + q_{\tilde{l}} \tag{3.2}$$

where $q_{\tilde{l}}$ defines additional timing offset per time slot and p represents the timing shift per block, in this case each combination $(p_{\tilde{l}}, q_{\tilde{l}})$ uniquely gives the positioning information of the coded signal from an interfering user. Note that in equation (3.2) in case $p_{\tilde{l}}$ and $q_{\tilde{l}}$ are integers and $p_{\tilde{l}} \in \{-N_2 + 1, ..., 0, ..., N_2 - 1\}$, $q_{\tilde{l}} \in \{-k_l + 1, ..., 0, ..., k_l - 1\}$, there are multiple access interferences in the system. We can easily see that when $\delta_{\tilde{l}} = \tau_l$ the interfering user has identical timing reference as the target signal does, thus

its spreaded signal will fully overlap with $\mathbf{Y}_l$ under the assumption that k_l is independent of the user index. For CTDMA-PWM the (j,i)th element of $\mathbf{Y}_l$ can be written as

$$\begin{aligned} Y_l[j,i] &= g_l[\frac{1-a_{j,l}}{2}H_{on,l}[i,i+1] \\ &+ \sum_{\tilde{l}:satisfying(3.2)} g_{\tilde{l}}[\frac{1-\tilde{a}_{j,\tilde{l}}}{2}H_{on,\tilde{l}}[i-q_{\tilde{l}},i+1-q_{\tilde{l}}]] \\ &+C_{dc}+v_{j,i} \end{aligned} \tag{3.3}$$

where $H_{on,l}[n_1,n_2]$ is the I&D processing of the Electro-Optical response function, which can be derived as $H_{on,l}[n_1,n_2]=\frac{\epsilon_l}{T_1}\int_{n_1T_1}^{n_2T_1}h_{on}(t)dt$. Hence

$$\begin{aligned} H_{on,l}[i,i+1] &= \frac{\epsilon_l}{T_1}\int_{iT_1}^{(i+1)T_1}(1-exp(-\frac{t}{\tau_{on}}))dt \\ &= \epsilon_l+\frac{\epsilon_l\tau_{on}}{T_1}[exp(-\frac{(i+1)T_1}{\tau_{on}})-exp(-\frac{iT_1}{\tau_{on}})] \end{aligned} \tag{3.4}$$

and

$$\begin{aligned} H_{on,\tilde{l}}[i-q_{\tilde{l}},i+1-q_{\tilde{l}}] &= \frac{\epsilon_l}{T_1}\int_{(i-q_{\tilde{l}})T_1}^{(i+1-q_{\tilde{l}})T_1}(1-exp(-\frac{t}{\tau_{on}}))dt \\ &= \epsilon_l+\frac{\epsilon_l\tau_{on}}{T_1}[exp(-\frac{(i+1-q_{\tilde{l}})T_1}{\tau_{on}})-exp(-\frac{(i-q_{\tilde{l}})T_1}{\tau_{on}})] \end{aligned} \tag{3.5}$$

In the equation (3.3), the variable $g_l=A_l\alpha_l\eta_l$ defines the individual light intensity from the lth LED at the sensor location and the parameter to be estimated in the project. The illumination pulse from other LEDs, background lights v_ς together with possible all **1** multiple access interference is denoted as the DC biased component C_{dc}. The noise term $v_{j,i}$ is Gaussian distributed with mean zero and variance $\sigma_v^2=\sigma_{th}^2+\sigma_{shot}^2$. Further, $\tilde{a}_{j,\tilde{l}}$ denotes the spreaded data sequence with p cyclic time shift, which can be written as:

$$\tilde{a}_{j,\tilde{l}}=\tilde{a}_{\tilde{l}}[j]=a_{\tilde{l}}[(j-p_{\tilde{l}}+N_2)\ mod\ N_2] \tag{3.6}$$

This is because in equation (2.3), the data resource is under our control thus we can use a 1 for every bit which leads to equation (2.4). Therefore, in case of asynchronous transmission, we will use a cyclic time shift of the desired spreading code to replace the processing of the target signal's previous or following bit provided that all 1 transmission bits are used.

From equation (3.3) , we can see that $\mathbf{Y}_l$ consists of the desired signal component, multiple access interference. DC bias term and Gaussian distributed noise. To apply a

linear MMSE detector, it is wise to vectorize equation (3.3), which is given by

$$\mathbf{y}_l = vec(\mathbf{Y}_l) = \begin{bmatrix} vec(\mathbf{H}_l) & vec(\mathbf{H}_{\tilde{l}_1}) & vec(\mathbf{H}_{\tilde{l}_2}) & \dots & vec(\mathbf{H}_{\tilde{l}_m}) \end{bmatrix} \begin{bmatrix} g_l \\ g_{\tilde{l}_1} \\ g_{\tilde{l}_2} \\ \vdots \\ g_{\tilde{l}_m} \end{bmatrix} + \mathbf{1}C_{dc} + \mathbf{v} \quad (3.7)$$

where $\mathbf{H}_l$ is the matrix with the (j,i)th element $H_l[j,i] = \frac{1-a_{j,l}}{2} H_{on\,l}[i, i+1]$. Likewise, $\mathbf{H}_{\tilde{l}_m}$ has the (j,i)th entry $H_{\tilde{l}_m}[j,i] = \frac{1-\tilde{a}_{j,\tilde{l}_m}}{2} H_{on,\tilde{l}_m}[i - q_{\tilde{l}}, i + 1 - q_{\tilde{l}}]$, in which m represents the amount of interfering users that cause the multiple access interference for the desired signal. $vec(\cdot)$ describes a linear transformation which converts the matrix into a column vector by stacking the columns of the matrix on top of one another. Specifically, the vectorization of the $N_2 \times k_l$ matrix $\mathbf{H}_l$, denoted by $vec(\mathbf{H}_l)$, is the $k_l N_2 \times 1$ column vector. Further, $\mathbf{v}$ is the vectorized noise term and $\mathbf{1}$ defines a vector with all the entries being equal to 1. Both $\mathbf{v}$ and $\mathbf{1}$ have the same dimension as $\mathbf{y}_l$, which is $k_l N_2 \times 1$. In order to have a standard LMMSE data model, we substitute $[\, vec(\mathbf{H}_l)\ vec(\mathbf{H}_{\tilde{l}_1})\ vec(\mathbf{H}_{\tilde{l}_2})\ \dots\ vec(\mathbf{H}_{\tilde{l}_m})]$ by $[\, \mathbf{h}_l\ \mathbf{h}_{\tilde{l}_1}\ \mathbf{h}_{\tilde{l}_2}\ \dots\ \mathbf{h}_{\tilde{l}_m}]$ and rewrite equation (3.7) as:

$$\mathbf{y}_l = \left[\begin{array}{cccccc} \mathbf{h}_l & \mathbf{h}_{\tilde{l}_1} & \mathbf{h}_{\tilde{l}_2} & \dots & \mathbf{h}_{\tilde{l}_m} & \mathbf{1} \end{array}\right] \begin{bmatrix} g_l \\ g_{\tilde{l}_1} \\ g_{\tilde{l}_2} \\ \vdots \\ g_{\tilde{l}_m} \\ - \\ C_{dc} \end{bmatrix} + \mathbf{v} \quad (3.8)$$

Hence

$$\mathbf{y}_l = \mathbf{H}\mathbf{g} + \mathbf{v} \quad (3.9)$$

where $\mathbf{H} = [\, \mathbf{h}_l\ \mathbf{h}_{\tilde{l}_1}\ \mathbf{h}_{\tilde{l}_2}\ \dots\ \mathbf{h}_{\tilde{l}_m}\ \mathbf{1}\,]$ with the dimension of $k_l N_2 \times (m+2)$ and $\mathbf{g} = [g_l \quad g_{\tilde{l}_1} \quad g_{\tilde{l}_2} \quad \dots \quad g_{\tilde{l}_m} \quad C_{dc}]^T$.

3.2 MMSE Linear Multiuser Detector

A common approach in estimation theory that can be applied to estimate the light intensity from the user of interest on the basis of the observing $\mathbf{y}_l$ is to apply a linear transformation $\mathbf{W}$ on $\mathbf{y}_l$ that minimizes the the Bayesian mean-square-error (MSE). This is so called linear minimum mean square error (LMMSE) estimation. We now consider all linear estimators of the form:

$$\hat{\mathbf{g}} = \mathbf{W}^T \mathbf{y}_l + \mathbf{w}_g \quad (3.10)$$

and minimize Bayesian MSE:

$$\mathrm{MSE}(\hat{\mathbf{g}}) = \mathbb{E}[\|\hat{\mathbf{g}} - \mathbf{g}\|^2] \quad (3.11)$$

Note that we have included the coefficient $\mathbf{w}_g$ since the input vector $\mathbf{g}$ and received vector $\mathbf{y}_l$ have both nonzero mean. In a classic communication system model, the signals that we want to transmit and estimate are normally zero mean, in this case, the coefficient $\mathbf{w}_g$ may be omitted. However, in this thesis, we are going to estimate the light intensity and apparently it has non-zero mean, therefore, $\mathbf{w}_g$ is included for an optimal solution. Now, we derive the optimal weighting coefficients matrix $\mathbf{W}$ and vector $\mathbf{w}_g$ for use in (3.10). Let us rewrite (3.11) by substituting (3.10) into (3.11)

$$\begin{aligned} \mathrm{MSE}(\hat{\mathbf{g}}) &= \mathbb{E}[\|\mathbf{W}^T\mathbf{y}_l - \mathbf{g} + \mathbf{w}_g\|^2] \\ &= \mathbb{E}[((\mathbf{W}^T\mathbf{y}_l - \mathbf{g}) + \mathbf{w}_g)^T((\mathbf{W}^T\mathbf{y}_l - \mathbf{g}) + \mathbf{w}_g)] \\ &= \mathbb{E}[\mathbf{w}_g^T\mathbf{w}_g + \mathbf{w}_g^T(\mathbf{W}^T\mathbf{y}_l - \mathbf{g}) + (\mathbf{W}^T\mathbf{y}_l - \mathbf{g})^T\mathbf{w}_g \\ &\quad +(\mathbf{W}^T\mathbf{y}_l - \mathbf{g})^T(\mathbf{W}^T\mathbf{y}_l - \mathbf{g})] \end{aligned} \tag{3.12}$$

and differentiate (3.12) with respect to $\mathbf{w}_g$

$$\bigtriangledown_{\mathbf{w}_g}\mathrm{MSE}(\hat{\mathbf{g}}) = \mathbb{E}[\mathbf{w}_g + \mathbf{W}^T\mathbf{y}_l - \mathbf{g}]$$

Setting this equal to zero produces

$$\mathbf{w}_g = \mathbb{E}[\mathbf{g}] - \mathbf{W}^T\mathbb{E}[\mathbf{y}_l] \tag{3.13}$$

which as indicated previously is zero if the mean of $\mathbf{g}$ and $\mathbf{y}_l$ are zero. Continuing, we need to minimize the Bayesian MSE, where $\mathbf{w}_g$ has been replaced by (3.13). Hence, the matrix $\mathbf{W}$ that minimizes

$$\mathrm{MSE}(\hat{\mathbf{g}}) = \mathbb{E}[\|\mathbf{W}^T(\mathbf{y}_l - \mathbb{E}[\mathbf{y}_l]) - (\mathbf{g} - \mathbb{E}[\mathbf{g}])\|^2] \tag{3.14}$$

must force the gradient to the zero matrix, that is

$$\mathbb{E}[(\mathbf{y}_l - \mathbb{E}[\mathbf{y}_l])(\mathbf{y}_l - \mathbb{E}[\mathbf{y}_l])^T\mathbf{W} - (\mathbf{y}_l - \mathbb{E}[\mathbf{y}_l])(\mathbf{g} - \mathbb{E}[\mathbf{g}])^T] = \mathbf{0} \tag{3.15}$$

Here we denote $\mathbb{E}[(\mathbf{y}_l - \mathbb{E}[\mathbf{y}_l])(\mathbf{y}_l - \mathbb{E}[\mathbf{y}_l])^T]$ as $\mathbf{C_{yy}}$ and $\mathbb{E}[(\mathbf{y}_l - \mathbb{E}[\mathbf{y}_l])(\mathbf{g} - \mathbb{E}[\mathbf{g}])^T]$ as $\mathbf{C_{yg}}$. $\mathbf{C_{yg}}$ represents the covariance of vector $\mathbf{y}_l$ and vector $\mathbf{g}$, and $\mathbf{C_{yy}}$ represents the variance of vector $\mathbf{y}_l$. Hence

$$\mathbf{W} = \mathbf{C}_{\mathbf{yy}}^{-1}\mathbf{C_{yg}} \tag{3.16}$$

To compute the right side of (3.16), we note that

$$\begin{aligned}
\mathbf{C_{yy}} &= \mathbb{E}[(\mathbf{y}_l - \mathbb{E}[\mathbf{y}_l])(\mathbf{y}_l - \mathbb{E}[\mathbf{y}_l])^T] \\
&= \mathbb{E}[(\mathbf{Hg} + \mathbf{v} - \mathbf{H}\mathbb{E}[\mathbf{g}])(\mathbf{Hg} + \mathbf{v} - \mathbf{H}\mathbb{E}[\mathbf{g}])^T] \\
&= \mathbb{E}[(\mathbf{H}(\mathbf{g} - \mathbb{E}[\mathbf{g}]) + \mathbf{v})(\mathbf{H}(\mathbf{g} - \mathbb{E}[\mathbf{g}]) + \mathbf{v})^T] \\
&= \mathbf{H}\mathbb{E}[(\mathbf{g} - \mathbb{E}[\mathbf{g}])(\mathbf{g} - \mathbb{E}[\mathbf{g}])^T]\mathbf{H}^T + \mathbb{E}[\mathbf{v}\mathbf{v}^T] \\
&= \mathbf{H}\mathbf{C_{gg}}\mathbf{H}^T + \sigma_v^2\mathbf{I} \qquad (3.17)
\end{aligned}$$

and

$$\begin{aligned}
\mathbf{C_{yg}} &= \mathbb{E}[(\mathbf{y}_l - \mathbb{E}[\mathbf{y}_l])(\mathbf{g} - \mathbb{E}[\mathbf{g}])^T] \\
&= \mathbb{E}[(\mathbf{Hg} + \mathbf{v} - \mathbf{H}\mathbb{E}[\mathbf{g}])(\mathbf{g} - \mathbb{E}[\mathbf{g}])^T] \\
&= \mathbf{H}\mathbb{E}[(\mathbf{g} - \mathbb{E}[\mathbf{g}])(\mathbf{g} - \mathbb{E}[\mathbf{g}])^T] \\
&= \mathbf{H}\mathbf{C_{gg}} \qquad (3.18)
\end{aligned}$$

where $\sigma_v^2 = \sigma_{th}^2 + \sigma_{shot}^2$ and $\mathbf{I}$ is the identity matrix. Therefore, the solution to (3.16) is given by

$$\begin{aligned}
\mathbf{W} &= (\mathbf{H}\mathbf{C_{gg}}\mathbf{H}^T + \sigma_v^2\mathbf{I})^{-1}\mathbf{H}\mathbf{C_{gg}} \\
&= (\mathbf{H}\mathbb{E}[(\mathbf{g} - \mathbb{E}[\mathbf{g}])(\mathbf{g} - \mathbb{E}[\mathbf{g}])^T]\mathbf{H}^T + \sigma_v^2\mathbf{I})^{-1}\mathbf{H}\mathbb{E}[(\mathbf{g} - \mathbb{E}[\mathbf{g}])(\mathbf{g} - \mathbb{E}[\mathbf{g}])^T] \qquad (3.19)
\end{aligned}$$

Using (3.13) and (3.19) in (3.10) produces

$$\begin{aligned}
\hat{\mathbf{g}} &= \mathbb{E}[\mathbf{g}] + \mathbf{W}^T(\mathbf{y}_l - \mathbb{E}[\mathbf{y}_l]) \\
&= \mathbb{E}[\mathbf{g}] + ((\mathbf{H}\mathbf{C_{gg}}\mathbf{H}^T + \sigma_v^2\mathbf{I})^{-1}\mathbf{H}\mathbf{C_{gg}})^T(\mathbf{y}_l - \mathbb{E}[\mathbf{y}_l]) \\
&= \mathbb{E}[\mathbf{g}] + \mathbf{C_{gg}}\mathbf{H}^T(\mathbf{H}\mathbf{C_{gg}}\mathbf{H}^T + \sigma_v^2\mathbf{I})^{-1}(\mathbf{y}_l - \mathbf{H}\mathbb{E}[\mathbf{g}]) \qquad (3.20)
\end{aligned}$$

where $\mathbf{C_{gg}} = \mathbb{E}[(\mathbf{g} - \mathbb{E}[\mathbf{g}])(\mathbf{g} - \mathbb{E}[\mathbf{g}])^T]$. Considering the lth LED as the user of interest, in order to estimate its intensity $\hat{g}_l$, we need to know the first element of the vector $\hat{\mathbf{g}}$

$$\hat{g}_l = (\mathbb{E}[\mathbf{g}] + \mathbf{C_{gg}}\mathbf{H}^T(\mathbf{H}\mathbf{C_{gg}}\mathbf{H}^T + \sigma_v^2\mathbf{I})^{-1}(\mathbf{y}_l - \mathbf{H}\mathbb{E}[\mathbf{g}]))^T \begin{bmatrix} 1 \\ 0 \\ 0 \\ \vdots \\ 0 \end{bmatrix}_{(m+2)\times 1} \qquad (3.21)$$

As we mentioned before, the parameter that we want to estimate is a bit different from the one in the conventional communication system, since in this project the light intensity that we aim to estimate is normally biased. To solve this problem, we need to statistically derive the mean and variance of the vector $\mathbf{g}$, which is denoted by $\mathbb{E}[\mathbf{g}]$ and $\mathbf{C_{gg}}$ in (3.21). For simplicity, we assume that the distance r_l between the lth LED and sensor is uniformly distributed, furthermore, the propagation distances from different LEDs to the sensor are independent. Due to the fact that $g_l = A_l\alpha_l\eta_l$ and $\alpha_l = \frac{1}{r_l^2}R(\phi_l)\mathcal{A}\cos(\psi_l)$ in (2.13), if other parameters are assumed to be fixed, g_l is proportional to $1/r_l^2$. Hence, we can say g_l is dependent on r_l. Now in case we have the probability distribution of r_l, both $\mathbb{E}[\mathbf{g}]$ and $\mathbf{C_{gg}}$ can be calculated. Recall equations (3.8) and (3.9), and we have $\mathbf{g} = [g_l \quad g_{\tilde{l}_1} \quad g_{\tilde{l}_2} \quad \dots \quad g_{\tilde{l}_m} \quad C_{dc}]^T$, therefore, $\mathbf{C_{gg}}$ is given by

$$\begin{aligned}\mathbf{C_{gg}} &= \mathbb{E}[(\mathbf{g}-\mathbb{E}[\mathbf{g}])(\mathbf{g}-\mathbb{E}[\mathbf{g}])^T] \\ &= \begin{bmatrix} \sigma_g^2 & 0 & \dots & 0 & 0 \\ 0 & \sigma_g^2 & \dots & 0 & 0 \\ \vdots & \vdots & \ddots & \vdots & \vdots \\ 0 & 0 & \dots & \sigma_g^2 & 0 \\ 0 & 0 & \dots & 0 & \sigma_{C_{dc}}^2 \end{bmatrix}\end{aligned} \tag{3.22}$$

From (3.22), it can be seen that $\mathbf{C_{gg}}$ is a diagonal matrix because each variable in the vector $\mathbf{g}$ is independent. Furthermore, all the entries except the last one in the vector $\mathbf{g}$ are identically distributed, therefore, σ_g^2 can be used to denote the variance of each element and $\sigma_g^2 = \mathbb{E}[(g_l - \mathbb{E}[g_l])^2]$. Note that $\sigma_{C_{dc}}^2$ in (3.22) represents the variance of the DC component C_{dc} in the data model (3.7) and (3.8). If C_{dc} is a constant value e.g. constant background light, $\sigma_{C_{dc}}^2$ becomes zero.

In order to implement the LMMSE estimator, we have to know the timing references and CDMA spreading codes from all users. To this end, let's assume that (p, q) of every LED is pre-defined and then the equation (3.3) is known so that the matrix $\mathbf{H}$ becomes deterministic. In this case, (3.21) estimates the light intensity of the desired LED.

Beyond the implementation of the LMMSE estimator, we may better understand the algorithm through rewriting the equation (3.20) as

$$\hat{\mathbf{g}} - \mathbb{E}[\mathbf{g}] = \mathbf{W}^T(\mathbf{y}_l - \mathbb{E}[\mathbf{y}_l]) \tag{3.23}$$

from which it is clearly seen that $\hat{\mathbf{g}} - \mathbb{E}[\mathbf{g}]$ and $\mathbf{y}_l - \mathbb{E}[\mathbf{y}_l]$ have zero mean, hence conventional MMSE solution $\mathbf{W}^T$ can be applied directly. Note that in (3.23), we intend to minimize the mean square error of $\hat{\mathbf{g}} - \mathbb{E}[\mathbf{g}]$ and $\mathbf{g} - \mathbb{E}[\mathbf{g}]$ instead of $\hat{\mathbf{g}}$ and $\mathbf{g}$ as in a conventional communication system. Again, what we are really interested is the first element of the vector $\mathbf{g}$. In order to estimate the intensity g_l, we need to know

the first column of the matrix $\mathbf{W}$, which is denoted as vector $\mathbf{w}_l$ that is given by

$$\mathbf{w}_l = (\mathbf{H}\mathbf{C}_{\mathbf{gg}}\mathbf{H}^T + \sigma_v^2\mathbf{I})^{-1}\mathbf{H}\mathbf{C}_{\mathbf{gg}} \begin{bmatrix} 1 \\ 0 \\ 0 \\ \vdots \\ 0 \end{bmatrix}_{(m+2)\times 1} \tag{3.24}$$

where $\sigma_v^2 = \sigma_{th}^2 + \sigma_{shot}^2$ and $\mathbf{I}$ is the identity matrix. By multiplying the row vector $[1, 0, 0, ..., 0]$ with the dimension $1\times$(m+2) to the left at both sides of the equality in (3.23), we will get

$$\hat{g}_l - \mathbb{E}[g_l] = \mathbf{w}_l{}^T(\mathbf{y}_l - \mathbb{E}[\mathbf{y}_l]) \tag{3.25}$$

Therefore, the intensity of the lth LED in the sensor location can be expressed as:

$$\hat{g}_l \;=\; \mathbb{E}[g_l] + \mathbf{w}_l{}^T(\mathbf{y}_l - \mathbb{E}[\mathbf{y}_l]) \tag{3.26}$$

from which we can see that substituting (3.24) into (3.26) produces exactly the same estimation result as in (3.21).

3.3 Blind Adaptive Multiuser Detector

3.3.1 Motivation

The conventional MMSE receiver needs to know the signature waveform and the timing of both desired user and interfering users. This requirement can not always be satisfied since in many cases we only have the knowledge of the signature waveform and the timing from the user of interest. For the considered asynchronous multiple access scheme, it is very difficult to get the information other than the desired LED. In addition, it is usually computationally intensive to carry out the inversion of the matrix with large dimension. Therefore, an adaptive algorithm which eliminates the need to know the spreading code and timing reference of the interfering LEDs can be very attractive.

One possible solution is to use the adaptive multiuser detector that is based on the minimization of the mean-square-error (MMSE) between the outputs and the data. For a survey of adaptive multiuser detection, please refer to [16] [17] [18] [19]. To apply adaptive MMSE detection, we need to know the training data sequence of the desired user. Here, the training sequence means a string of data known to the receiver in the initial phase of running the algorithm. The transmitter sends a set of training symbols at start-up which the receiver uses for initial adaptation. After the training phase ends, the adaptive detector learns the filter impulse response while adaptation during actual data occurs in decision-directed mode. The advantage of the adaptive MMSE detector is its ability to have fully asynchronous transmission, while the disadvantage is its dependence on the constancy of the interfering environment and the prerequisite to know the training sequence. In our project, one of the major objectives is to estimate

the lighting intensity by using multiuser detection techniques. However, in order to apply the adaptive MMSE detector, we need to first train the data sequence of lighting intensity. This is not feasible since we don't have full knowledge of the lighting intensity even in the initial phase. As a result, the adaptive MMSE detector is not fully compatible to the proposed lighting system.

Motivated by the analysis above, in this section, we will investigate the blind adaptive multiuser detection to combat the multiple access interference without requiring the training sequence. Actually, this blind multiuser detector requires no more knowledge than the conventional single user receiver does, namely desired spreading code and its timing reference.

3.3.2 Canonical Representation

The blind approach is based on the decomposition of the linear multiuser detector as the sum of two orthogonal components. One of those components is the vector $\mathbf{h}_l$, which is indeed the first column of matrix $\mathbf{H}$ in the equation (3.9) and it is assumed to be known and fixed in the algorithm. The other component $\mathbf{x}_l$, orthogonal to $\mathbf{h}_l$, is a variable vector and the target that we want to estimate by using the adaptive algorithm. In order to derive the formula of the blind adaptive MMSE detection, it is valuable to introduce the aforementioned canonical representation for the linear multiuser detector of the lth LED:

$$\mathbf{w}_l = \mathbf{h}_l + \mathbf{x}_l \tag{3.27}$$

In addition to equation (3.27), the orthogonality is guaranteed by

$$\mathbf{h}_l^T \mathbf{x}_l = 0 \tag{3.28}$$

(3.27) and (3.28) effectively constrain the overall impulse response of the desired user to a constant

$$\begin{aligned} \mathbf{w}_l^T \mathbf{h}_l &= (\mathbf{h}_l^T + \mathbf{x}_l^T)\mathbf{h}_l \\ &= \|\mathbf{h}_l\|^2 \end{aligned} \tag{3.29}$$

Here we rule out the possibility that the linear transformation is orthogonal to $\mathbf{h}_l$, since they result in an error probability equal to 1/2. Note that $\mathbf{h}_l$ is a column vector with a length of $k_l N_2$ and it includes the component $\frac{1-a_{j,l}}{2}$ in each of the elements. In case we use balanced "1" and "-1" WH code, the vector $\frac{\mathbf{1}-\mathbf{a}_l}{2}$ has balanced "0" and "1", thus the norm of this vector equals $N_2 k_l/2$, where $\mathbf{a}_l$ represents the k_l stacked spreading codes under the assumption of (2.4). If the on- and off-switching times τ_{on} and τ_{off} are much smaller that the time slot T_1, the on and off ramp becomes negligible so that

$$\|\mathbf{h}_l\|^2 = \frac{k_l N_2 \epsilon_l}{2} \tag{3.30}$$

The following subsection will show that equations (3.27) and (3.28), resulting into equation (3.29), are the constraints imposed to force the receiver to converge to the user of interest. In case $\mathbf{h}_l$ is assumed to be known, $\mathbf{x}_l$ needs to be estimated by minimizing a certain cost function.

3.3.3 Minimum Output Energy Linear Detector

The linear transformation $\mathbf{w}_l$ of the received signal is typically designed by minimizing a certain cost function. In this subsection, I repeat equation (3.25) as a starting point to derive the related results

$$\hat{g}_l - \mathbb{E}[g_l] = {\mathbf{w}_l}^T(\mathbf{y}_l - \mathbb{E}[\mathbf{y}_l]) \tag{3.31}$$

One classical approach that is derived in section 3.2 adopts the mean-square-error (MSE) between $g_l - \mathbb{E}[g_l]$ and $\hat{g}_l - \mathbb{E}[g_l]$ using the equation (3.31)

$$\begin{aligned} \mathrm{MSE}(\mathbf{w}_l) &= \mathbb{E}[((g_l - \mathbb{E}[g_l]) - (\hat{g}_l - \mathbb{E}[g_l]))^2] \\ &= \mathbb{E}[((g_l - \mathbb{E}[g_l]) - \mathbf{w}_l^T(\mathbf{y}_l - \mathbb{E}[\mathbf{y}_l]))^2] \end{aligned} \tag{3.32}$$

When a blind solution is desired, an output-only criterion is sought. In the absence of the noise, the optimization of this cost function under certain conditions will yield a decorrelating solution, while in the presence of the noise, the result will converge to the MMSE solution. In this subsection, we name the output-only cost function as mean-output-energy (MOE) or output variance of the linear transformation. Thus the approach is called linear minimum output energy (MOE) detector or linear minimum output variance detector (MOVD). In our data model (3.31), what we intend to minimize is the mean output energy of $\hat{g}_l - \mathbb{E}[g_l]$, which can be given by:

$$\mathrm{MOE}(\mathbf{x}_l) = \mathbb{E}[(\mathbf{w}_l^T(\mathbf{y}_l - \mathbb{E}[\mathbf{y}_l]))^2] = \mathbb{E}[((\mathbf{h}_l + \mathbf{x}_l)^T(\mathbf{y}_l - \mathbb{E}[\mathbf{y}_l]))^2] \tag{3.33}$$

It is shown below that $\mathbf{x}_l$ which minimizes MOE also minimizes MSE. In other words, through the following derivation, we can say linear MMSE detector is nothing else but a linear MOE detector plus a constant value.

$$\begin{aligned} \mathrm{MSE} &= \mathbb{E}[((g_l - \mathbb{E}[g_l]) - (\mathbf{h}_l + \mathbf{x}_l)^T(\mathbf{y}_l - \mathbb{E}[\mathbf{y}_l]))^2] \\ &= \mathrm{MOE}(\mathbf{x}_l) + \mathbb{E}[(g_l - \mathbb{E}[g_l])^2] - 2\mathbb{E}[(g_l - \mathbb{E}[g_l])^2](\mathbf{h}_l + \mathbf{x}_l)^T\mathbf{h}_l \\ &= \mathrm{MOE}(\mathbf{x}_l) + (1 - 2\|\mathbf{h}_l\|^2)\mathbb{E}[(g_l - \mathbb{E}[g_l])^2] \end{aligned} \tag{3.34}$$

By knowing this, we may rewrite the equation (3.33) as:

$$\mathrm{MOE}(\mathbf{x}_l) = \mathbf{w}_l^T \mathbf{C}_{yy} \mathbf{w}_l \tag{3.35}$$

where $\mathbf{C}_{yy} = \mathbb{E}[(\mathbf{y}_l - \mathbb{E}[\mathbf{y}_l])(\mathbf{y}_l - \mathbb{E}[\mathbf{y}_l])^T]$. It is clear from (3.35) that the cost function is minimized for $\mathbf{w}_l = 0$. In order to avoid the trivial solution, we propose to minimize MOE cost function under constraints (3.27) and (3.28). This is also motivated because for any linear transformation we want to put some energy into the desired response $\mathbf{h}_l$ and force the linear transformation of the desired response to be a constant value, which can be verified by (3.29). Under these conditions, by using a certain recursive optimization algorithm, the multiple access interference due to other undesired channel responses will be canceled, thus the result will converge to the conventional MMSE solution.

The method we use to self-tune the detector is gradient decent or steepest descent of a convex penalty function. It is also well known as the Least Mean Squares (LMS) algorithm. Although other faster minimization strategies may also be applicable, in my thesis, we will focus on LMS optimization algorithms for simplicity.

3.3.4 Blind Adaptation 1

In this section, we investigate an adaptive version of the proposed method using an instantaneous approximation of the gradient. The derivation of the adaptation rule for $\mathbf{x}_l[i]$ is very simple. The unconstrained gradient of the averaged random variable in

$$\mathrm{MOE}(\mathbf{x}_l) = \mathbb{E}[((\mathbf{h}_l + \mathbf{x}_l)^T (\mathbf{y}_l - \mathbb{E}[\mathbf{y}_l]))^2]$$

is equal to a scaled version of the observations

$$\bigtriangledown \mathrm{MOE}(\mathbf{x}_l) = 2((\mathbf{h}_l + \mathbf{x}_l)^T (\mathbf{y}_l - \mathbb{E}[\mathbf{y}_l]))(\mathbf{y}_l - \mathbb{E}[\mathbf{y}_l]) \tag{3.36}$$

In order to restrict the search direction in the constrained space, it is important to fulfill the orthogonality condition (3.28) at each step of the algorithm, therefore we use the projection of the gradient of the unconstrained output energy MOE ($\mathbf{x}_l$) onto the linear subspace orthogonal to $\mathbf{h}_l$. Note that the steepest descent line along the subspace orthogonal to $\mathbf{h}_l$ is the projection of the gradient on that subspace.The unconstrained gradient can be decomposed as the sum of its projections along $\mathbf{h}_l$ and its orthogonal subspace; steepest descent requires steepest descent in each of those directions. Based on the analysis above, we need to project the vector $\mathbf{y}_l - \mathbb{E}[\mathbf{y}_l]$ onto the subspace orthogonal to $\mathbf{h}_l$, which is given by:

$$\begin{aligned} (\mathbf{y}_l - \mathbb{E}[\mathbf{y}_l])_{\mathbf{h}_l}^{\perp} &= (\mathbf{I} - \frac{1}{\|h_l\|^2} \mathbf{h}_l \mathbf{h}_l^T)(\mathbf{y}_l - \mathbb{E}[\mathbf{y}_l]) \\ &= (\mathbf{y}_l - \mathbb{E}[\mathbf{y}_l]) - \frac{1}{\|h_l\|^2} (\mathbf{h}_l^T (\mathbf{y}_l - \mathbb{E}[\mathbf{y}_l])) \mathbf{h}_l \end{aligned} \tag{3.37}$$

Since $\bigtriangledown$MOE is a scaled version of $\mathbf{y}_l - \mathbb{E}[\mathbf{y}_l]$, the projected gradient of MOE can be easily written as

$$\bigtriangledown \text{MOE}(\mathbf{x}_l)^{\perp}_{\mathbf{h}_l} = 2(\mathbf{h}_l + \mathbf{x}_l)^T(\mathbf{y}_l - \mathbb{E}[\mathbf{y}_l])((\mathbf{y}_l - \mathbb{E}[\mathbf{y}_l]) - \frac{1}{\|h_l\|^2}(\mathbf{h}_l^T(\mathbf{y}_l - \mathbb{E}[\mathbf{y}_l]))\mathbf{h}_l) \quad (3.38)$$

The adaptive algorithm updates the process at the data rate. The observed waveform is slotted into different waveforms, where i represents the iteration time.

$$...\mathbf{y}_l[i-1], \mathbf{y}_l[i], \mathbf{y}_l[i+1]...$$

and the orthogonal component at the ith iteration, x[i], depends on

$$...\mathbf{y}_l[i-1], \mathbf{y}_l[i]$$

Furthermore, we can collect the received signal y_l and calculate its averaged value $\mathbb{E}[\mathbf{y}_l])$ after a large number of iterations. Hence, at each iteration, we use the update direction $\bigtriangledown \text{MOE}(\mathbf{x}_l)^{\perp}_{\mathbf{h}_l}$ and then the stochastic gradient adaptation rule is

$$\mathbf{x}_l[i] = \mathbf{x}_l[i-1] - \lambda(\mathbf{h}_l + \mathbf{x}_l[i-1])^T(\mathbf{y}_l[i] - \mathbb{E}[\mathbf{y}_l])\{(\mathbf{y}_l[i] - \mathbb{E}[\mathbf{y}_l]) - \frac{1}{\|h_l\|^2}(\mathbf{h}_l^T(\mathbf{y}_l[i] - \mathbb{E}[\mathbf{y}_l])\mathbf{h}_l)\} \quad (3.39)$$

where λ is the step size of the update process.

3.3.5 Blind Adaptation 2

In this subsection, we will propose a different approach to achieve the blind solution. We may first rewrite equation (3.26) with subject to the constraints (3.27) and (3.28)

$$\hat{g}_l = \mathbf{w}_l{}^T\mathbf{y}_l + b = (\mathbf{h}_l + \mathbf{x}_l)^T\mathbf{y}_l + b \quad (3.40)$$

where $b = \mathbb{E}[g_l] - \mathbf{w}_l{}^T\mathbb{E}[\mathbf{y}_l]$, which also needs to be estimated in this approach. MOE is given by

$$\text{MOE} = ((\mathbf{h}_l + \mathbf{x}_l)^T\mathbf{y}_l)^2 + 2b(\mathbf{h}_l + \mathbf{x}_l)^T\mathbf{y}_l + b^2 \quad (3.41)$$

In this equation, we have two unknown parameters $\mathbf{x}_l$ and b, which can both be estimated using LMS algorithm. To this end, we differentiate (3.41) with respect to b and $\mathbf{x}_l$, respectively

$$\bigtriangledown_b \text{MOE} = 2b + 2(\mathbf{h}_l + \mathbf{x}_l)^T\mathbf{y}_l \quad (3.42)$$

and

$$\begin{aligned} \bigtriangledown_{\mathbf{x}_l} \text{MOE} &= 2((\mathbf{h}_l + \mathbf{x}_l)^T \mathbf{y}_l)\mathbf{y}_l + 2b\mathbf{y}_l \\ &= 2((\mathbf{h}_l^T + \mathbf{x}_l^T)\mathbf{y}_l + b)\mathbf{y}_l \end{aligned} \tag{3.43}$$

Using LMS algorithm in (3.42) produces

$$b[i] = b[i-1] - \lambda(b[i-1] + (\mathbf{h}_l^T + \mathbf{x}_l^T[i-1])\mathbf{y}_l[i]) \tag{3.44}$$

Next, we also project the vector $\mathbf{y}_l$ onto the subspace orthogonal to $\mathbf{h}_l$, which is given by

$$\begin{aligned} \mathbf{y}_{l\mathbf{h}_l}^{\perp} &= (\mathbf{I} - \frac{1}{\|h_l\|^2}\mathbf{h}_l\mathbf{h}_l^T)\mathbf{y}_l \\ &= \mathbf{y}_l - \frac{1}{\|h_l\|^2}(\mathbf{h}_l^T\mathbf{y}_l)\mathbf{h}_l \end{aligned} \tag{3.45}$$

hence, the projected gradient of MOE can also be written as

$$\bigtriangledown \text{MOE}(\mathbf{x}_l)_{\mathbf{h}_l}^{\perp} = 2((\mathbf{h}_l^T + \mathbf{x}_l^T)\mathbf{y}_l + b)(\mathbf{y}_l - \frac{1}{\|h_l\|^2}(\mathbf{h}_l^T\mathbf{y}_l)\mathbf{h}_l) \tag{3.46}$$

Using LMS algorithm in (3.43) produces

$$\mathbf{x}_l[i] = \mathbf{x}_l[i-1] - \lambda((\mathbf{h}_l^T + \mathbf{x}_l^T[i-1])\mathbf{y}_l[i] + b[i])(\mathbf{y}_l[i] - \frac{1}{\|h_l\|^2}(\mathbf{h}_l^T\mathbf{y}_l[i])\mathbf{h}_l) \tag{3.47}$$

Equations (3.44) and (3.47) give the result of $\mathbf{x}_l$. Conceptually, the approach presented in Blind Adaptation 2 is better than the previous one in Blind Adaptation 1, since we don't need to collect received signal and calculate its expected value, which will save time for us to running the algorithm.

3.4 Numerical Result

In this section, we will perform the Matlab simulation based on the data model and estimation algorithm we apply in the proposed system. In order to analyze the numerical results, subsection 3.4.1 specifies different system parameters in one typical scenario. Afterwards, the result of conventional MMSE and blind adaptive MMSE linear detectors will be presented in the subsequent subsections.

3.4.1 Simulation Parameter

Let's consider a scenario of a typical large indoor environment of 10m×10m with approximately hundreds LEDs. For the simplicity of both the LED array fabrication and

algorithm implementation, we assume that the illumination LEDs are uniformly distributed in the ceiling in a square grid. The receiving sensor is assumed to be located in the middle of the room, hence it's shortest distance to the ceiling is the height, and we assume it is 1m. Table 3.1 gives parameters of channel disturbance as well as parameters of lamps and sensors.

Table 3.1: Simulation Parameters of Lamps, Sensor and Channel Disturbance

Parameters	Values
Background light power	$5\text{w}/m^2$
PSD of electron noise, S_{th}	$1.69 \times 10^{-24} A^2/Hz$
Lambertian mode number μ	1,2,5
Responsivity of LED η	1W/A
Responsivity of photodiode ϵ	0.3217W/A
Area of the PD, $\mathcal{A}$	$10^{-4}m^2$
Switching speed of LED, τ_{on}, τ_{off}	$0.02 \times 10^{-6}s$
LED output power A_l	0.5-5 W

From the table, we can obtain the background noise in the PD receiver which is $5\text{w}/m^2 \times 10^{-4}m^2 = 5 \times 10^{-4}\text{w}$. Moreover, the Lambertian mode number μ is the same for all LEDs. The switching Speed of LED is set to be $0.02 \times 10^{-6}s$, therefore, it is much smaller than one slot period, hence the on- and off- ramp effect can be neglected. The parameters in the table can be considered as pre-defined such that these parameters are constant as the system is well configured.

In table 3.2, we can see a number of system parameters which can be adjusted for the better estimation performance and the desired lighting effect.

Table 3.2: Simulation System Parameters

Parameters	Values
Time slot duration T_1	$10^{-6}s$
Length of the block N_1	32
Length of the spreading code N_2	32
Timing reference of the desired signal τ_l	2
Modulation depth k_l	2
Duty cycle of each LED pp_l	50%

It can be seen from the table that Walsh-Hadamard codes with the length $N_2 = 32$ are randomly assigned to different users. In conventional MMSE algorithm, we assume that all the codes are pre-known to different users. In blind MMSE approach, only the code for the user of interest is desired. The length of one block is set to be 32 so that the dimming level equals 5bits. The slot period $T1 = 10^{-6}s$, which ensures $\tau_{on} \ll T_1$ and $\tau_{off} \ll T_1$. Moreover, every LED takes $k_l = k = 2$ slots for modulation and they all operate at the same duty cycle of 50%. Although all the LEDs emit the coded light in the same time, in our simulation, we only consider the sensing performance through the light "link c" between one LED and the sensor.

In the simulation, we use the normalized MSE (N-MSE) performance to assess the

accuracy of the light intensity estimation. Normalized MSE is derived by the squared value of MSE and actual light intensity. We shows N-MSE results as a function of distance between any LED to the sensor r_l, where $r_l = \sqrt{h^2 + x_l^2 + y_l^2}$ with (x_l, y_l) the ceiling grid coordinates the light source with respect to the sensor. In one estimation algorithm, we assume sensor is fixed and we take the numerical results for LED at different locations on the ceiling.

3.4.2 Simulation Result

Figure 3.1 and 3.2 depict the normalized MSE (N-MSE) in light intensity as a function of distance, for different value of A_l and μ. respectively. It is shown from the figures that the performance in intensity estimation degrades in an exponential fashion as the distance between the LED and sensor increases. From Figure 3.1, it is also clearly shown that we can achieve better performance with larger LEDs output power. This is not difficult to understand because in case we increase A_l, the SNR is accordingly increased.

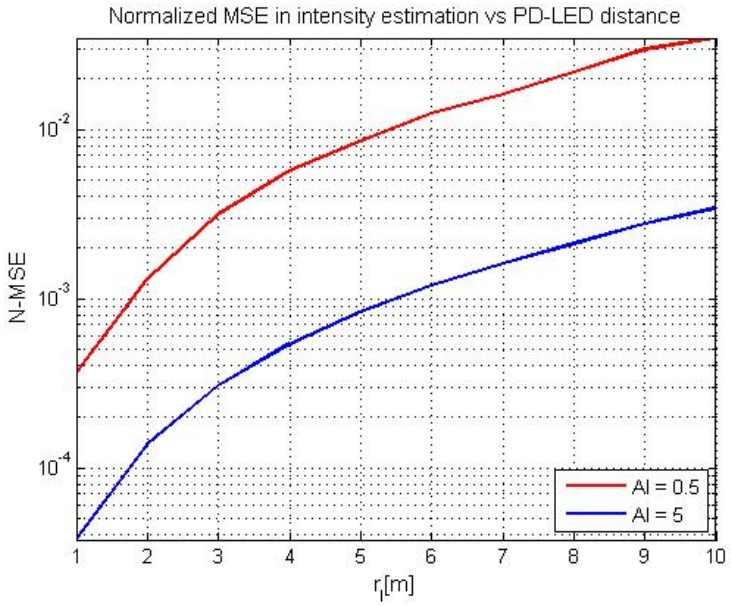

Figure 3.1: Normalized MSE in intensity estimation vs. PD-LED distance with variable A_l

Figure 3.2 describes similar results for $A_l = 5$ with different radiation patterns, for $\mu = 1, 2, 5$. We can observe that we get considerable estimation error, $\mathrm{N-MSE} < 10^{-2}$, in intensity estimation using LMMSE estimator.

In the following, we will show the results of blind adaptive MMSE linear estimator. It can be seen that the blind result converges to MMSE solution after sufficient iteration times. Note that in these simulations, we take $A_l = 5$ and $\mu = 1$ as an example.

Figure 3.3 gives the blind result in the case that the step size $\lambda = 10^8$ and iteration time equals 10000. Note that $r_l = 1$ in this result. From the figure, we can see that

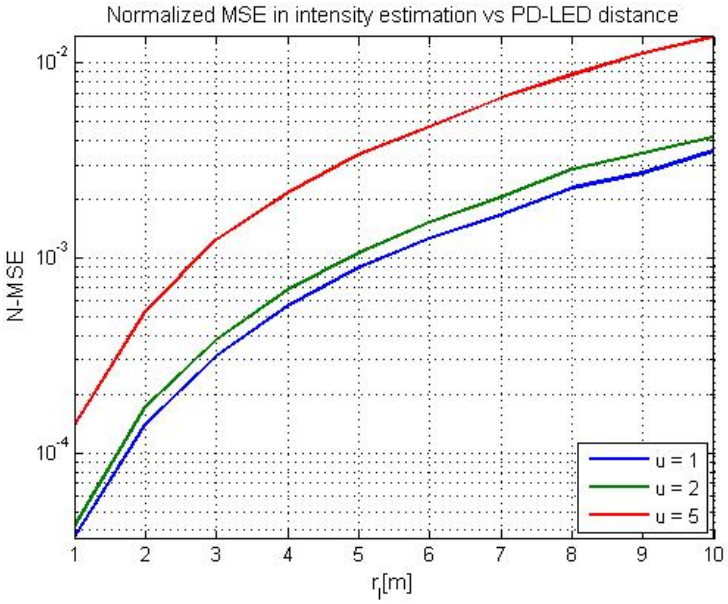

Figure 3.2: Normalized MSE in intensity estimation vs. PD-LED distance with variable μ

N-MSE converges after approximately 2000 times iteration. Therefore, the time spent to measure one LED is $T_1 \times N_1 \times N_2 \times IterationTime < 2s$

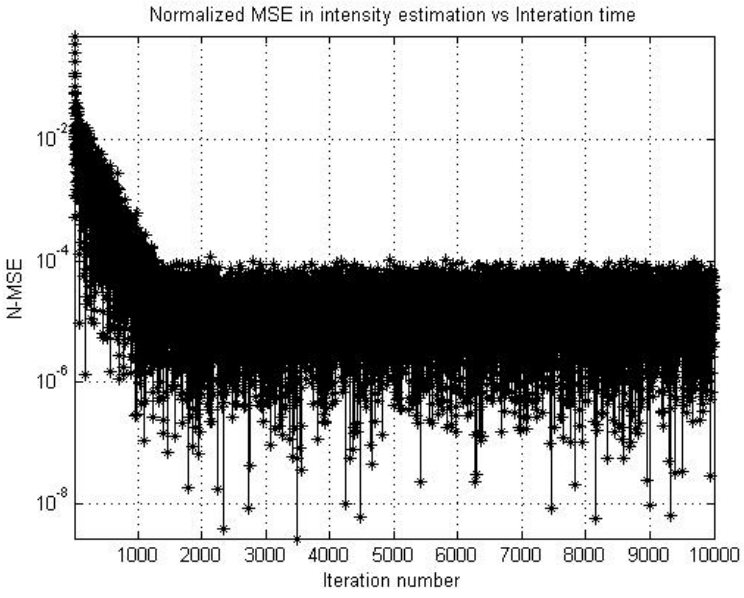

Figure 3.3: Normalized MSE in intensity estimation vs. iteration time with $\lambda = 10^8, r_l = 1$

Figure 3.4 shows another result of the blind MMSE estimator when the step size $\lambda = 2 \times 10^8$ and iteration time equals 10000, from which we can see the blind estimator

converges faster than the the previous one does. This is simply because we twice the step size. On the other hand, it can be observed that the result presents more ups and downs, but the performance result is more or less the same. We can conclude that we get a trade off between convergence speed and stability by choose appropriate step size.

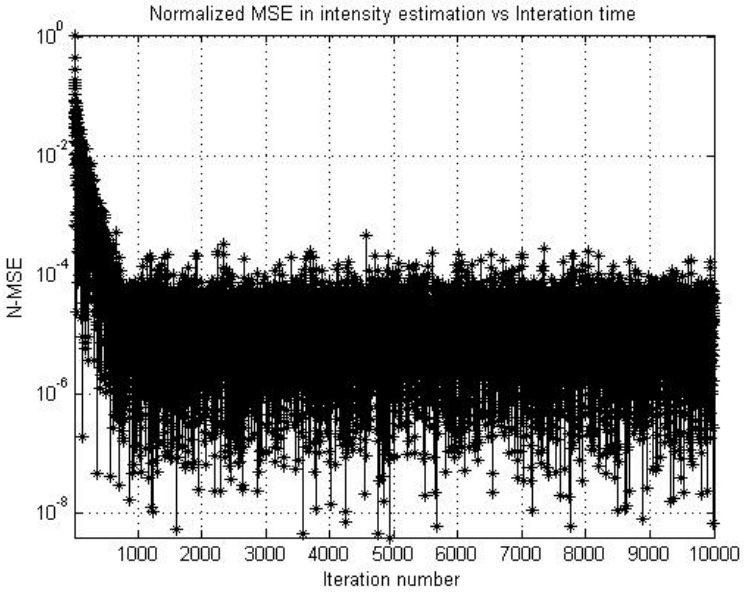

Figure 3.4: Normalized MSE in intensity estimation vs. iteration time with $\lambda = 2\times10^8, r_l = 1$

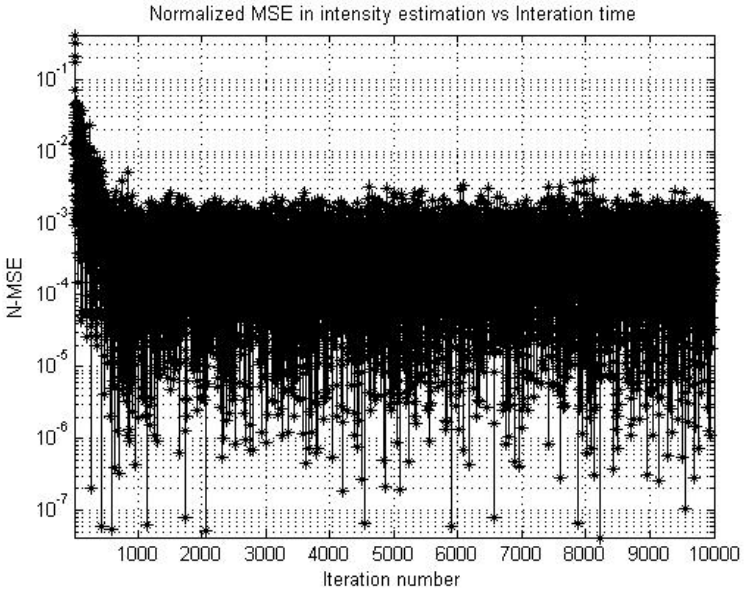

Figure 3.5: Normalized MSE in intensity estimation vs. iteration time with $\lambda = 2\times10^{11}, r_l = 5$

Figure 3.5 depicts the normalized MSE in light intensity of a blind estimator with the parameter $\lambda = 10^8$ and $r_l = 1$. The result coincides the results we got in Figure 3.1 and and Figure 3.2. In case r_l increases, performance in intensity estimation degrades. Note that in this simulation, step size $\lambda = 10^{11}$ which is much larger than the previous value we took. This is because the norm square of the received vector $\mathbf{y}_l$ decreases accordingly.

3.5 Conclusion

This chapter is the major contribution of my master thesis. It derives the receiver data model in section 3.1. Afterwards, the conventional MMSE and Blind MMSE algorithms are investigated. The result shows that Blind MMSE estimator converges to an acceptable N-MSE performance with appropriate update step size and sufficient iteration time. For a large room scenario considered in this chapter, we propose an asynchronous CTDMA-PWM scheme with corresponding multiuser detection algorithms. By using the parameter we considered in section 3.4, we conclude that each LED can be measured within a 2s period and hundreds of LEDs can be estimated accurately and simultaneously.

4 Imaging Diversity

In this chapter, I will present some basic study and research for a new idea of imaging diversity to provide an optical solution for the aforementioned problems. Basically, we use a imaging sensor with multiple pixels to separately receive the signal from different LEDs. In this way, signal from different LEDs can be fully or partially distinguished.

As shown in Figure 4.1, L (here $L = 5$) LED lamps are located on the ceiling separated by a distance d. We order L (odd number) lamps from 1, 2, 3 to L and put corresponding coordinates nearby. A circular thin lens, a lens of negligible thickness, with a radius of R is placed u meter from the ceiling. An imaging receiver is put n meter from the lens to receive the projection of the lights from lamps.

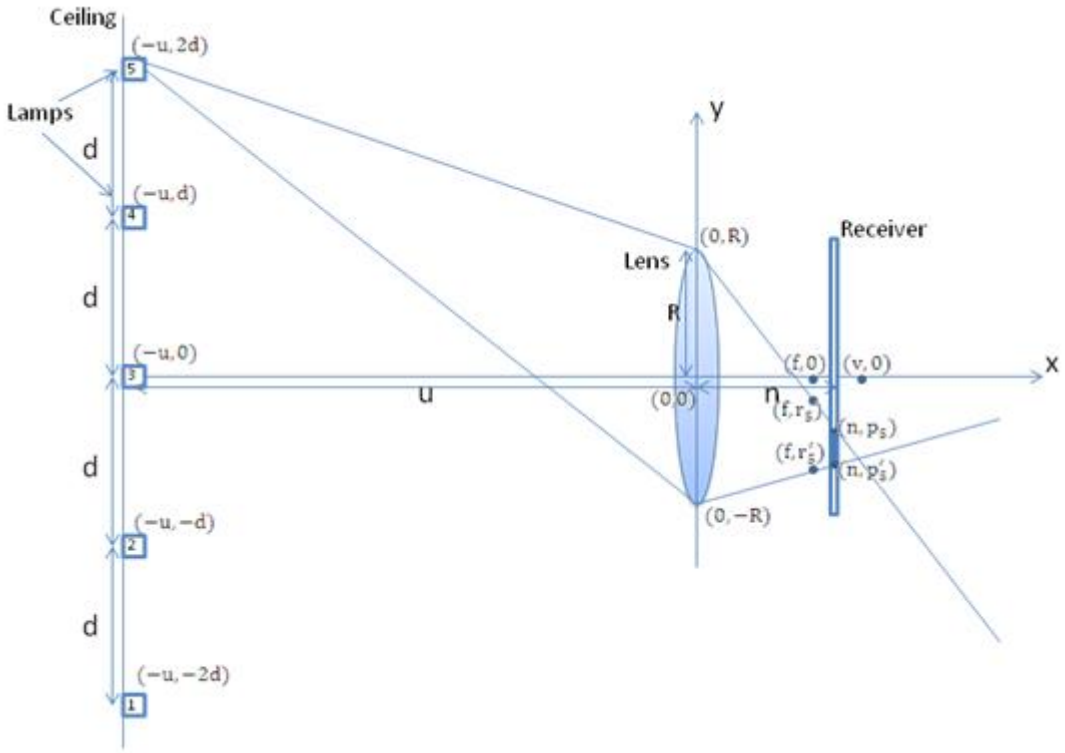

Figure 4.1: Model for lens design

If the distance from the object to the lens and from the lens to the image is u and v respectively, the distances are related by the thin lens formula:

$$\frac{1}{v} + \frac{1}{u} = \frac{1}{f} \tag{4.1}$$

where f represents the focal length of the lens. Consider the special situation that the

imaging receiver is put f meters far from the lens, which means $n = f$, the top of the projection r_m of the mth lamp is given by:

$$r_m = \frac{f}{u}[-(m - \frac{L+1}{2})d + R] \tag{4.2}$$

where $m \in \{1, 2, ..., N\}$. Likewise, the bottom of the projection can be derived as:

$$r_m{}' = \frac{f}{u}[-(m - \frac{L+1}{2})d - R] \tag{4.3}$$

When $|r_m| \geq |r_{m-1}{}'|$, e.g. $\frac{f}{u}(d - 2R) \geq 0$, there is no overlap of the projections of lamp m and lamp $m - 1$. Therefore, when $n = f$, the non-overlap condition is given by:

$$d \geq 2R \tag{4.4}$$

In the following, we present the results from Matlab simulations when $d = 2R$ and $d = R$ in the left and right figure respectively. It can be seen that when $d = R$ there is overlap, but when $d = 2R$, the projections touch but there is no overlap.

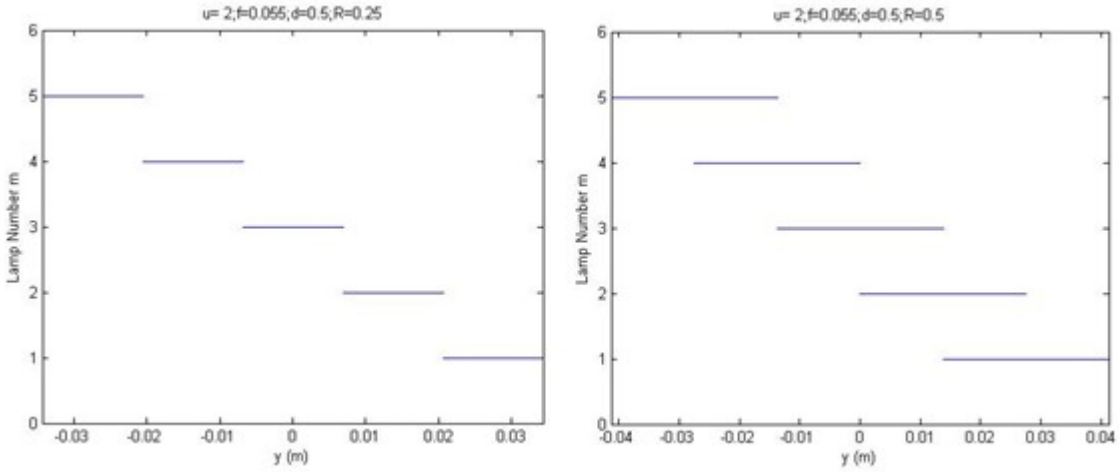

Figure 4.2: overlapping criterion when $n = f$

Normally, the lens will be much smaller, hence we choose $R = 0.01m$, which is far less than the distance between two lamps. Therefore, there is never overlap when we put the receiver in the focal point of the lens. Figure 4.3 shows the projection distribution when $f = 0.055m$, $d = 0.5m$ and $R = 0.01m$, which are very practical parameters. Apart from the projection of each lamp, It is also important to know the size of the total projection. It could be easily derived by the following formula:

$$|r_1| \geq |r_L{}'| = \frac{f}{u}[(L-1)d + 2R] \tag{4.5}$$

From Figure 4.1, it can be seen that $(L-1)d$ represents the size of the ceiling, and in practice, $2R$ is much smaller than $(L-1)d$, hence the size of the total projection equals $\frac{f}{u}$ times the size of the ceiling.

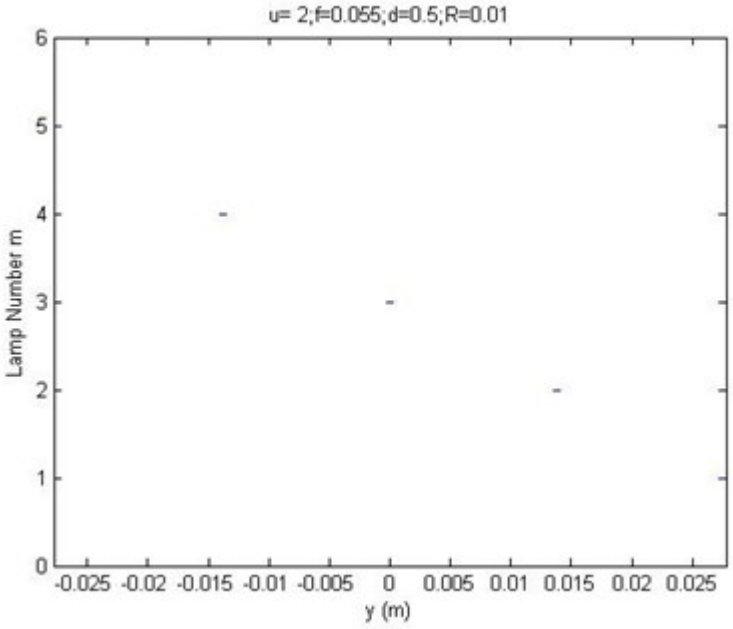

Figure 4.3: Typical projection distribution when $n = f$

Next, let's consider the case that the distance between the lens and the imaging receiver n is a variable from 0 to positive infinity. According to the geometric relations, the top s_m and bottom $s_m{}'$ of the projections can be shown to be the following:

$$s_m = R - \frac{n}{f}(R - r_m) \tag{4.6}$$

$$s_m\prime = \frac{n}{f}(R + r_m) - R \tag{4.7}$$

where $m \in \{1, 2, ..., N\}$. Substituting (4.2) and (4.3) into (4.6) and (4.7) respectively, we obtain

$$s_m = R - \frac{n}{f}\{R - \frac{f}{u}[-(m - \frac{N+1}{2})d + R]\} \tag{4.8}$$

$$s_m{}' = \frac{n}{f}\{R + \frac{f}{u}[-(m - \frac{N+1}{2})d - R]\} - R \tag{4.9}$$

Figure 4.4 shows the projection distribution when n varies from 0 to $4f$. The graph shows that when $n = 0$ the projections from each lamp are completely overlapped, when n increases to a certain value p , the projections touch each other but there is no overlap. Afterwards, the size of the projection will decrease to a point when $n = v = uf/(u - f)$, and then it keeps increasing as n becomes larger until the next stage that n reaches another value q where the projections touch each other but there

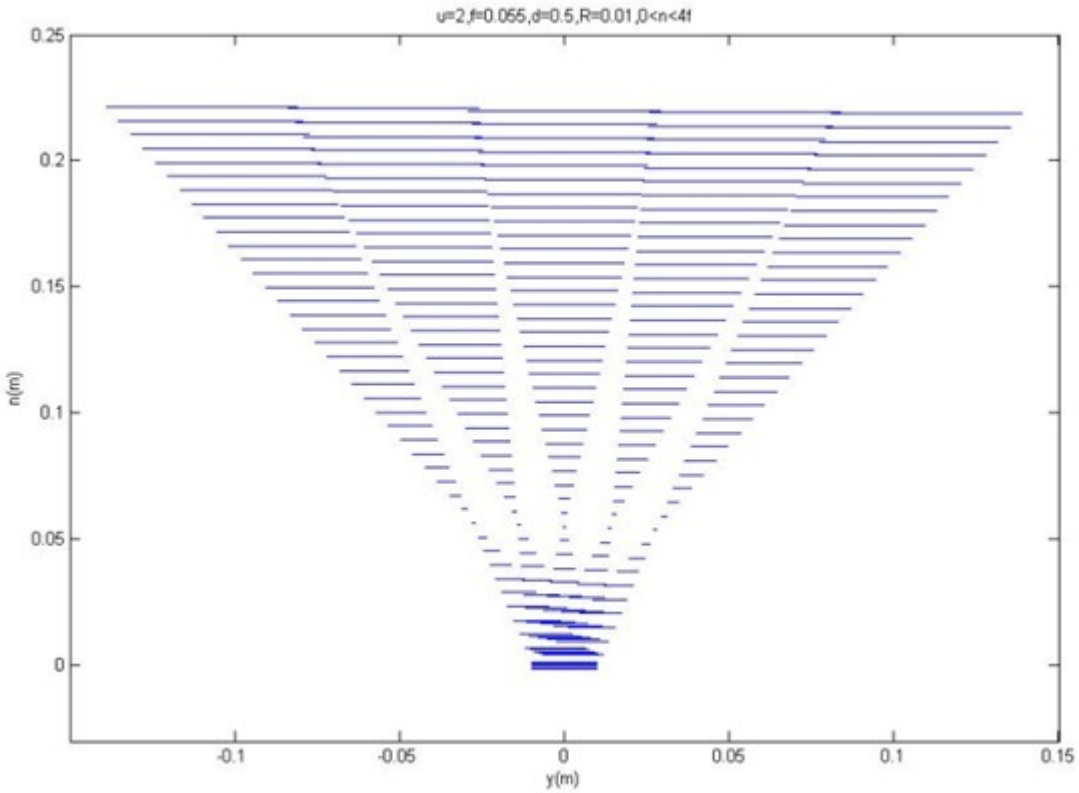

Figure 4.4: Typical projection distribution when n is a variable

is no overlap. We can imagine that when n goes to infinity, the projections from each lamp will become infinitely large and fully overlapped.

So it would be valuable to limit n within the range of (p, q) to guarantee the non-overlapping. Considering the criterion that $|s_m| \geq |s_{m-1}{}'|$ or $|s_{m-1}| \leq |s_m{}'|$, which can be given by:

$$\frac{2R}{f} + \frac{d-2R}{u}n \geq 2R \tag{4.10}$$

$$\frac{2R}{f} - \frac{d+2R}{u}n \leq 2R \tag{4.11}$$

Therefore, we can make a conclusion that

$$p = (\frac{2R}{f} + \frac{d-2R}{u}n)^{-1}2R \tag{4.12}$$

$$q = (\frac{2R}{f} - \frac{d+2R}{u}n)^{-1}2R \tag{4.13}$$

In addition, the size of the total projection comes to the following formula:

$$|{s_1}' - s_N| = 2R - \frac{n}{f}2R + \frac{n}{u}(N-1)d + \frac{n}{u}2R \tag{4.14}$$

From Figure 4.4, we can see that by choosing appropriate parameters, the projection in the pixel can be fully or partially separated.

5 Conclusion

In this chapter we summarize the work done in the thesis, draw the final conclusions, and suggest directions for further research.

5.1 Conclusion

In this thesis, we have first given an overview of an intelligent lighting control system. Its basic idea, major application, working principle and system architecture are introduced. In addition, the main drawbacks of a synchronous transmission system are presented, which motivate us to perform the research on an asynchronous multiple access scheme. Finally, we outline the main content of each chapter and summarize our contribution to the entire project in Philips Research.

Chapter 2 mainly discusses the data model of the proposed system. Pulse width modulation (PWM) and code-time division multiple access (CTDMA) are studied to allow multiple LEDs to access the sensor receiver simultaneously and distinguish the light sources individually within the aggregate illumination. To this end, a three layer modulation structure is introduced, through which pulse width modulation is performed within each block and CDMA scheme is processed within one frame. Furthermore, we analyze the problem of the synchronous transmission system and propose the asynchronous multiple access scheme. Although the asynchronous CTDMA system doesn't strictly require perfect synchronization, it gives a big advantage in the transmission design. However, it brings the problem of multiple access interference (MAI) that needs to be suppressed at the receiver by using advanced signal processing algorithms, which will of course increase the complexity of the receiver design. In this chapter, the problem is clearly illustrated and is treated as a preparation for the possible solution in Chapter 3 and Chapter 4. Finally, three major channel disturbances of this visible light link are modeled and the received CTDMA-PWM signals are derived analytically.

In Chapter 3, we first derive the data model of the asynchronous receiver. Afterwards, we assume to have all the information about channel input and apply the conventional MMSE linear detector to give a solution. However, due to the fact that we may not know the timing reference and spreading code from other LEDs, this solution will not be very useful in the practical situation. Therefore, we propose to use a blind adaptive linear detector, which requires no more knowledge than the conventional single user receiver does. In case we know the spreading code and its timing reference from the user of interest, by using the least mean squares (LMS) algorithm, we can recursively minimize the cost function of the mean output energy (MOE) instead of the mean square error (MSE). The result shows that blind MMSE converges and achieves an acceptable N-MSE performance with appropriate update step size and sufficient iteration time.

Finally, Chapter 4 gives some basic results of the lens design for the imaging diversity method.

5.2 Suggestions for Future Work

- In section 3.2, a blind adaptive MMSE linear multiuser detector is presented, where the Least Mean Squares (LMS) algorithm is used to iteratively search a Wiener solution for the minimum output energy. However, other potentially faster techniques can also be applied in lieu of LMS, for instance, Recursive Least Squares (RLS). Therefore, I think it is a good idea to use the RLS algorithm as an alternative solution for a faster convergence speed.

- With the blind adaptive MMSE receiver, we don't fully use the knowledge of the channel input. Hence, it might be a good idea to use the Multiple Signal Classification (MUSIC) algorithm to estimate the timing offset of every asynchronous spreading code. These can be combined with the knowledge of the spreading code to estimate the desired parameter by using the conventional MMSE algorithm. Since we have a clear description of channel input, the performance is expected to be improved considerably.

- In Chapter 4, basic idea of imaging diversity is proposed with the use of an array of pixels in the imaging sensor. However, in my thesis, I only present basic lens design. This can be further extended to a deeper research. We may put it in the channel model, in case we cannot achieve complete separation, partial separation can decrease the computational intensity for the receiver algorithm considerably.

Bibliography

[1] Jean-Paul M.G. Linnartz; Lorenzo Feri; Hongming Yang; Sel B. Colak; Tim C.W. Schenk, "Communications and sensing of illumination contributions in a power led lighting system," *IEEE International Conference on Communications (ICC 2008)*, pp. 5396–5400, May 2008.

[2] Pu Li; Tim C.W. Schenk; Ronald Rietman, "Framed random access for reliable light source identification in smart lighting systems," *Symposium IEEE Benelux Chapter on Communications and Vehicular Technology 2009 (SCVT2009)*, Nov. 2009.

[3] Jean-Paul M.G. Linnartz; Lorenzo Feri; Hongming Yang; Sel B. Colak; Tim C.W. Schenk, "Code division-based sensing of illumination contributions in solid-state lighting systems," *IEEE Transactions on Signal Processing*, vol. 57, no. 10, pp. 3984–3998, Sep. 2009.

[4] Tim C.W. Schenk; Lorenzo Feri; Hongming Yang; Jean-Paul M.G. Linnartz, "Optical wireless cdma employing solid-state lighting leds (invited)," *IEEE Photonics Society Summer Topicals 2009*, pp. 23–24, Jul. 2009.

[5] Luxeon Star LEDs, "http://www.luxeonstar.com/faqs.php," .

[6] J. M. H. Elmirghani and R. A. Cryan, "New ppm-cdma hybrid for indoor diffuse infrared channels," *Electronics Letters*, vol. 30, pp. 1646–1647, Sep. 1994.

[7] U. N. Griner and S. Arnon, "Multiuser diffuse indoor wireless infrared communications using equalized synchronous cdma," *IEEE Transactions Communication*, vol. 54, pp. 1654–1662, Sep. 2006.

[8] M. Z. Afgani; H. Haas; H. Elgala; and D. Knipp, "Visible light communication using ofdm," *Tridentcom 2006*, vol. 54, pp. 1654–1662, Mar. 2003.

[9] D. Wood, *Optoelectronic Semiconductor Devices*, Prentice Hall, 1994, ch. 1,2,3,5,6.

[10] A. Descombes and W. Guggenbuhl, "Investigation of the influence of several diode parameters on the light-delay time in large-area shjunction led's," *IEEE Transactions Electron Devices*, vol. ED-25, no. 3, pp. 379–382, Mar. 1978.

[11] A. Descombes and W. Guggenbuhl, "Large signal circuit model for led's used in optical communication," *IEEE Transactions Electron Devices*, vol. ED-28, no. 4, pp. 395–404, Apr. 1981.

[12] Pouyan Djahani and Joseph M. Kahn, "Analysis of infrared wireless links employing multibeam transmitters and imaging diversity receivers," *IEEE Transactions on Communications*, vol. 48, no. 12, Dec. 2000.

[13] F. R. Gfeller and U. Bapst, "Wireless in-house communication via diffuse infrared radiation," *IEEE*, vol. 67, no. 11, pp. 1474–1486, Nov. 1979.

[14] A. E. Iverson and D. L. Smith, "Mathematical modeling of photoconductor transient response," *IEEE Transactions Electron Devices*, vol. 34, pp. 2098–2107, Oct. 1987.

[15] J. M. Kahn and J. R. Barry, "Wireless infrared communications," *IEEE*, vol. 85, no. 2, pp. 265–298, Feb. 1997.

[16] Sergio Verd, *Multiuser Detection*, The Press Syndicate of The University of Cambridge, 1998.

[17] Sergio Verd Michael Honig, Upamanyu Madhow, "Blind adaptive multiuser detection," *IEEE Transactions on Information Theory*, vol. 41, no. 4, Jul. 1995.

[18] Michail K. Tsatsanis, "Inverse filtering criteria for cdma systems," *IEEE Transactions on Signal Processing*, vol. 45, no. 1, Jan. 1997.

[19] S. Haykin, *Adaptive Filter Theory*, Prentice-Hall, 1991.